To the Graduate Council:

I am submitting herewith a thesis written by Ziran Sun entitled "Mathematical Modeling of Glucose Utilization and 2,5-Diketo-D-Gluconic Acid Concentration in Batch Fermentation Using *Pantoea citrea*." I have examined the final copy of this thesis for form and content and recommend that it can be accepted in partial fulfillment of the requirements for the degree of Master of Science, with a major in Chemical Engineering.

Paul Frymier, Major Professor

We have read this thesis
and recommend its acceptance:

Accepted for the Council:

Associate Vice Chancellor and
Dean of the Graduate School

Mathematical Modeling of Glucose Utilization and 2,5-Diketo-D-Gluconic Acid Production in Batch Fermentation Using *Pantoea citrea*

A Thesis

Presented for the

Master of Science

Degree

The University of Tennessee, Knoxville

Ziran Sun

August, 1999

Copyright © Ziran Sun, 1999

All rights reserved

DEDICATION

My eternal gratitude to my parents Dr. Yian Sun and Mrs. Xin Zhou who have both given up so much for me, and to whom I wholeheartedly dedicate this body of work

Acknowledgments

I would like to first and foremost thank my parents, Dr. Yian Sun and Mrs. Xin Zhou. They both could have led a very comfortable life in China. But in order to provide a better life and more opportunities for me, they came to America. Enduring many years of hardship and numerous personal sacrifices, they have to the utmost of their abilities provided me with the best they have to offer. Without their tremendous patience and hard working ethics, I would not have arrived here today.

I would like to acknowledge Dr. Giuseppe Pizzorno, of the Department of Medical Oncology at Yale University Medical School, for showing me what research in the life sciences was like. I would like to thank my advisor, Dr. Paul Frymier, for not only believing in me and providing me an opportunity to enter into graduate school to reaffirm myself academically but also his insights and the endless hours spent editing this draft. I would like to thank Dr. Gary Saylor of the Center for Environmental Biotechnology not only for his financial support, but also his vast knowledge and caring attitude, two characteristics found rarely in the same person. An enormous debt of gratitude goes to Dr. Christine Kelly (Department of Chemical Engineering, Syracuse University) for her trust and her recommendation to the CEB.

I would like to thank the following people for their contributions in the completion of this work: Dr. Charles Moore for being on my committee, Matt Dalton for his analytical works, Dr. Justin Shingleton for his persistence in never giving up on ideas, and Dr. John Sanseverino for providing his vast knowledge on the Microbiology aspect of this work. Finally, I would like to thank the following people who have had a

tremendous contribution in shaping me into who I am today: Professors Kenneth Ackley (Department of Chemical Engineering, Cornell University) and his wife Miriam, Professor Barry Shain (Department of Political Science, Colgate University) and his wife and daughter, Carolyn and Susan, Janine Leffert and Earle Adams in Dr. Pizzorno's lab, Greg Trass, Bob States, and Dr. Margarete Hachigian at Innovation Packaging Corporation, my cohorts at www.cyber-m.com, Gary Williams and John Peterson, and everyone and everything that I may have inadvertently neglected.

Abstract

The experimental and mathematical analyses in this study have furthered knowledge in batch production of 2,5-diketo-gluconic acid by *Pantoea citrea* (ATCC 37410). This study was driven by three objectives: (a) to derive a mathematical model based on Michaelis-Menten enzyme kinetics to describe the batch production of 2,5-DKG, (b) to investigate the role central cellular metabolism played in the batch production of 2,5-DKG, and (c) to compare the relative activity of the major internal pathways for glucose catabolism.

Central carbon metabolism, growth rates, and cell yields were determined in *P. citrea* using glucose, fructose, gluconate, or pyruvate as growth substrates. Key enzymatic activities of the Embden-Meyerhoff-Parnas (EMP), Entner-Douderoff (ED), and pentose phosphate (PP) pathways were examined using *Escherichia coli* as a reference. All cells were grown on minimal medium containing 28mM glucose, fructose, gluconate, or pyruvate at 28 C. The cell yield on glucose was 0.089 compared to 0.17 for fructose or gluconate. Cells grown on glucose achieved half the concentration of those grown on fructose. The key EMP enzyme, phosphofructokinase, showed a low activity (0.21 units/mg protein) relative to *E. coli* (0.42 units/mg protein). 6-phosphogluconate dehydratase and KDPG aldolase, two key enzymes of the ED pathway, also showed lower activities in *P. citrea* than in *E. coli*. 6-phosphogluconate dehydrogenase, the key enzyme of the pentose phosphate pathway, exhibited a higher activity in *P. citrea* than in *E. coli*. 2-keto-gluconate dehydrogenase, a membrane-bound enzyme in *P. citrea*, was

also assayed. Results show a high level of activity for 2-ketogluconate dehydrogenase. The low activity of phosphofructokinase, coupled with poor growth rate on glucose, and high activity of the membrane-bound dehydrogenases suggested that the glucose is channeled through the outer membrane dehydrogenases and thus prevented from entering central metabolism in *P. citrea.*

Batch productions using both viable and nonviable cells were performed to show the effect of central metabolism on the batch production of 2,5-DKG. Batch runs with viable cells yielded a final conversion of glucose to 2,5-DKG of 73% in 10 hours. Two forms of nonviable cells were used: (1) cellular membrane fractions obtained by lysing viable cells using a French press, yielding 70% conversion in 12 hours and (2) permeabilized cells obtained by exposure to toluene, yielding over 90% conversion in 20 hours. While elimination of central metabolism by permeabilization of the cells resulted in an overall higher overall conversion from glucose to 2,5-DKG, the time it took to reach the final conversion was much longer. However, elimination of central metabolism by French pressing the cells did not result in an overall conversion,

A mathematical model based on the Michaelis-Menten kinetics of the three oxidation enzymes responsible for 2,5-DKG production glucose dehydrogenase, gluconate dehydrogenase, and 2-KDG dehydrogenase, was developed to describe the 2,5-DKG concentration profile in the batch case. Kinetic parameters for each of these dehydrogenases were determined experimentally.

The model consisted of a set of 4 coupled, nonlinear ordinary differential equations, each one describing the concentration of a species involved in the 2,5-DKG

pathway. The input parameters needed were the volumetric activities of each enzymes, glucose dehydrogenase (E1), gluconate dehydrogenase (E2), and 2-KDG dehydrogenase (E3), cell density (X), and a glucose uptake rate constant, U_T. Of these parameters, only the volumetric E3 activity and cell density were measurable. The other three parameters were determined by fitting the experimental data for one case of batch experiments performed with whole cells. These fit parameters were volumetric E1 activity = volumetric E2 activity = volumetric E3 activity, and U_T = 0.08 mmol/g/min. This model, with the fit parameters, successfully predicted the 2,5-DKG profile from another experiment with whole cells.

A sensitivity analysis on how the overall conversion of glucose to 2,5-DKG (79 %) and time required to reach that nominal conversion (11 hr) would change with perturbations in the volumetric activities of E1 and E2, and U_T revealed that small perturbations of the volumetric activities of E1 and E2, and U_T did not affect greatly either the overall nominal conversion of glucose to 2,5-DKG or the amount of time required to achieve that conversion. The overall nominal conversion was most sensitive to perturbations in the volumetric E1 activity and U_T, and the time required to achieve the nominal conversion was most sensitive to the perturbations in the volumetric E2 activity.

Table of Content

1 Introduction 1

1.1 The Reichstein Process 2

1.2 Bacterial Bioprocesses for Ascorbic Acid Synthesis 3

1.3 Purpose 6

2 Objectives 7

3 Literature Review 8

3.1 Overview 8

3.2 Central Metabolism 10

3.2.1 Glucose Transport 11

3.2.2 The Embden-Meyerhof-Parnas (EMP) Pathway 12

3.2.3 The Entner-Douderoff (ED) Pathway 13

3.2.4 The Pentose Phosphate (PP) Pathway 14

3.3 Extracellular Degradation of Glucose 14

3.3.1 Bioconversion of Glucose to 2,5-DKG 15

3.3.2 Glucose Dehydrogenase 16

3.3.3 Gluconate Dehydrogenase 16

3.3.4 2-KDG Dehydrogenase 17

3.4 Summary of Glucose Metabolic Pathways in *P. citrea* 17

3.5 Enzyme Mechanisms 19

3.6 Michaelis-Menten Enzyme Kinetics 20

3.7 Lineweaver-Burk Plots 24

4 Materials and Methods 25

4.1 Materials 25

4.2 Frozen Stock Preparation 25
4.3 Preparation of Cell Free Extract for Intracellular Enzyme Assays 26
4.4 Intracellular Enzyme Assays 27
4.4.1 6-Phosphoglyconate Dehydrogenase 29
4.4.2 6-Phosphogluconate dehydratase and KDPG aldolase 30
4.4.3 Phosphofructokinase 31
4.5 Extracellular Enzyme Assays 32
4.5.1 Glucose Dehydrogenase 32
4.5.2 Gluconate Dehydrogenase 34
4.5.3 2-KDG Dehydrogenase 35
4.6 Protein Determination 36
4.7 Batch Experiments 36
4.7.1 Cell Growth for Batch Experiments 37
4.7.2 Preparations of Nonviable Cells 37
4.8 Analytical Methods 38
5 Mathematical Model Studies 40
5.1 Mathematical Model for the Batch Production of 2,5-DKG 40
5.1.1 Mass Balance on Glucose 40
5.1.2 Mass Balance on Gluconate 43
5.1.3 Mass Balance on 2-KDG 44
5.1.4 Mass Balance on 2,5-DKG 44
5.2 Determination of Kinetic Parameters 45
5.2.1 Kinetic Parameters for Glucose Dehydrogenase 45
5.2.2 Kinetic Parameters for Gluconate Dehydrogenase 47
5.2.3 Kinetic Parameters for 2-KDG Dehydrogenase 49
6 Results 55

6.1 Growth Characteristics of *P. citrea* 55

6.2 Enzyme Activities of *P. citrea* and *E. coli* in Log Phase 58

6.3 Enzyme Activities of *P. citrea* in Stationary Phase 60

6.4 Batch Production of 2,5-DKG 61

6.4.1 Batch production of 2,5-DKG using whole cells of P. citrea *62*

6.4.2 Batch production of 2,5-DKG using French-pressed P. citrea cells *64*

6.4.3 Batch production of 2,5-DKG using permeabilized P. citrea cells *69*

7 Mathematical Modeling of 2,5-DKG Concentration Profile **76**

7.1 Modeling 2,5-DKG Concentration in the Whole Cell Batch Experiment (the Low Concentration Case) 77

7.1.1 Sensitivity Analysis for the Model Parameter Volumetric E1 Activity *79*

7.1.2 Sensitivity Analysis for the Model Parameter E2 Activity *81*

7.1.3 Sensitivity Analysis for the Model Parameter U_T *83*

7.2 Modeling 2,5-DKG Concentration in the Whole Cell Batch Experiment (High Cell Concentration) 86

7.3 Modeling 2,5-DKG Concentration in Batch Experiments Using Nonviable Cells 88

8 Conclusions **92**

BIBLIOGRAPHY **95**

VITA **98**

List of Figures

Figure 3-1 Glucose utilization pathways associated with cellular central metabolism 9

Figure 3-2 Summary of major pathways of glucose metabolism and the key enzyme(s) involved in each pathway 18

Figure 3-3 A plot of the reaction velocity as a function of the substrate concentration [S] for an enzyme obeying Michaelis-Menten kinetics 21

Figure 4-1 The sharp rise (indicated by the arrow) in % dissolved oxygen after 10 hours of growth, indicating the beginning of stationary phase 28

Figure 5-1 The enzymatic model schematic and the kinetics proposed 41

Figure 5-2 Lineweaver-Burk plot for initial-rate experiments conducted with two enzyme concentrations of glucose dehydrogenase, obtained from *Bacillus megaterium* 46

Figure 5-3 Comparison of experimentally measured velocities and predicted velocities using parameters derived from Lineweaver-Burk plot at glucose dehydrogenase concentration of 2.5 U/mL 48

Figure 5-4 Comparison of experimentally measured velocities and predicted velocities using parameters derived from Lineweaver-Burk plot at glucose dehydrogenase concentration of 1.25 U/ml 48

Figure 5-5 Lineweaver-Burk plot for initial-rate experiments conducted with two enzyme concentrations of gluconate dehydrogenase, obtained from *Pseudomonas sp.* 50

Figure 5-6 Comparison of experimentally measured velocities and predicted velocities using parameters derived from Lineweaver-Burk plot at gluconate dehydrogenase concentration of 1.25 U/m 51

Figure 5-7 Comparison of experimentally measured velocities and predicted velocities using parameters derived from Lineweaver-Burk plot at gluconate dehydrogenase concentration of 0.625 U/m 51

Figure 5-8 Lineweaver-Burk plot for initial-rate experiments conducted with two enzyme concentrations of 2-KDG dehydrogenase, from *Pantoea citrea* 53

Figure 5-9 Comparison of experimentally measured velocities and predicted velocities using parameters derived from Lineweaver-Burk plot at 2-KDG dehydrogenase concentration of 18.9 U/m 54

Figure 5-10 Comparison of experimentally measured velocities and predicted velocities using parameters derived from Lineweaver-Burk plot at 2-KDG dehydrogenase concentration of 11.9 U/m 54

Figure 6-1 Optical density and cell concentration (mg dw/ml) for *P. citrea* 56

Figure 6-2 Growth curve of *P. citrea* on various carbohydrate substrates 57

Figure 6-3 Glucose and 2,5-DKG concentration profiles in batch experiments using whole cells (volumetric 2-KDG dehydrogenase activity = 15.95 U/mL) 63

Figure 6-4 Glucose and 2,5-DKG concentration profiles in batch experiments using whole cells (volumetric 2-KDG dehydrogenase = 24.6 U/mL) 65

Figure 6-5 Glucose and 2,5-DKG concentration profiles in batch experiments using French-pressed cells (volumetric 2-KDG dehydrogenase activity = 19.05 U/mL) 67

Figure 6-6 Cross section schematic of a French press cell chamber 70

Figure 6-7 Glucose and 2,5-DKG concentration profiles in batch experiments using permeabilized cells (volumetric 2-KDG dehydrogenase activity = 22.43 U/mL) 72

Figure 6-8 Sigmoidal dependence of reaction velocity on substrate concentration [S] for an allosteric enzyme 74

Figure 7-1 Experimental 2,5-DKG concentration profiles from batch experiment using whole cells and model fit using parameters: volumetric E1 activity = volumetric E2 activity = volumetric E3 activity = 19.45 U/mL, and U_T = 0.08 mmol/g/min 78

Figure 7-2 The effects of perturbations in the volumetric E1 activity on the overall conversion of glucose to 2,5-DKG and the time required to reach nominal conversion of 79% 80

Figure 7-3 The effects of perturbations in the volumetric E2 activity on the overall conversion of glucose to 2,5-DKG and the time required to reach nominal conversion of 79% 82

Figure 7-4 The effects of perturbations in U_T (in mmol/g/min)on the overall conversion of glucose to 2,5-DKG and the time required to reach nominal conversion of 79% 85

Figure 7-5 Experimental 2,5-DKG concentration profiles from batch experiment using whole cells and model fit using parameters: volumetric E1 activity = volumetric E2 activity = volumetric E3 activity = 24.6 U/mL, and U_T = 0.08 mmol/g/min 87

Figure 7-6 Experimental 2,5-DKG concentration profiles from batch experiment using French-pressed cells and model fit using parameters: volumetric E1 activity = volumetric E2 activity = volumetric E3 activity = 19.05 U/mL, and U_T = 0 mmol/g/min 89

Figure 7-7 Experimental 2,5-DKG concentration profiles from batch experiment using permeabilized cells and model fit using parameters: volumetric E1 activity = volumetric E2 activity = volumetric E3 activity = 22.43 U/mL, and U_T = 0 mmol/g/min 90

List of Tables

Table 3-1 Major pathways and associated key enzyme(s) for glucose metabolism 19

Table 5-1 Experimentally Determined Kinetic Parameters for the Enzymes in 2,5-DKG Production Pathway 52

Table 6-1 Growth Characteristics of *P. citrea* on Various Carbohydrates 58

Table 6-2 Relative Activities of Internal Metabolic Pathways in *P. citrea* in Growth Phase Grown on Various Carbohydrates 59

Table 6-3 Relative Activities of Internal Metabolic Pathways in *E. coli* in Growth Phase Grown on Various Carbohydrates 59

Table 6-4 Relative Activities of Internal Metabolic Pathways in *P. citrea* in Stationary Phase with Various Air Flow Rates 60

Table 6-5 Volumetric 2-KDG Dehydrogenase Enzyme Activity and Protein Concentration at the Beginning and End of Batch Production of 2,5-DKG Using Whole Cells 62

Table 6-6 Volumetric 2-KDG Dehydrogenase Enzyme Activity and Protein Concentration at the Beginning and End of Batch Production of 2,5-DKG Using French-pressed Cells 68

Table 6-7 Volumetric 2-KDG Dehydrogenase Enzyme Activity and Protein Concentration at the Beginning and End of Batch Production of 2,5-DKG Using Permeabilized Cells 71

Table 7-1 Result of Perturbation of the Volumetric Glucose Dehydrogenase (E1) Activity on the Overall Conversion of Glucose to 2,5-DKG and Time Required for Nominal Conversion 81

Table 7-2 Result of Perturbation of Gluconate dehydrogenase (E2) Activity on the Conversion of Glucose to 2,5-DKG and Time Required for Nominal Conversion 83

Table 7-3 Result of Perturbation of Glucose Uptake Rate Constant (U_T) on the Overall Conversion of Glucose to 2,5-DKG and Time Required for Nominal Conversion 84

1 Introduction

L-Ascorbic acid is produced mainly in the food and drug industries. It is an essential part of diet. Its primary function is to regenerate the enzyme catalyzing the reaction for the hydroxylation of proline residues in collagen. Ascorbic acid reduces the ferric ion of the inactivated enzyme prolyl hydroxylase, and in turn is itself oxidized to dehydroascorbic acid. Thus ascorbic acid serves as a specific antioxidant. Studies reveal that collagen synthesized in vitro in the absence of ascorbic acid has a lower melting temperature than does the normal protein. Furthermore, dietary deficiency disease such as scurvy may occur in the absence of ascorbic acid (Stryer, 1995).

During the last ten years, ascorbic acid production has steadily increased, with a growth rate of 2 to 3 percent. In 1998, the United States production reached 40 million pounds. The projected growth is 3 percent per year through the year 2002. Hoffman - La Roche, the leading manufacturer of ascorbic acid in the United States, plans to spend over $200 million in the next four years to improve production technology at its largest ascorbic acid production site in Dalry, Scotland. A joint venture involving BASF, Merck, and Cerestar will use jointly developed fermentation technology to reduce costs of ketogluconic acid, a key intermediate in the synthesis of ascorbic acid, at a new facility in Krefeld, Germany in late 1999. The Archer Daniels Midland Company (ADM) plans to have ascorbic acid production from its Decatur plant in 1999. A consortium of chemical and biotechnology companies, led by Genecor International, is in current

development of a process starting with glucose that yields ketogluconic acid after a series of enzymatic reactions. The intermediate is then converted to ascorbic acid through conventional chemistry. The traditional route of ascorbic acid synthesis is the Reichstein process; however, emphasis in recent years has been on reducing the cost of production by improving the technology (Chem Profile, 1999).

1.1 The Reichstein Process

Traditional synthesis of ascorbic acid is through the Reichstein process, which requires the bioconversion of sorbitol. There are five steps involved. The first step is the reduction of glucose to sorbitol through the use of a nickel catalyst. The second step is the oxidation of sorbitol to sorbose, which may be performed through fermentation using *Acetobacter suboxydans*. The third step is a treatment with acetone and sulfuric acid to produce diacetone sorbitol. The fourth step is the oxidation of diacetone sorbitol to 2-keto-L-gulonate (2-KLG) through the use of a platinum catalyst. The final step is the enolization and internal lactonization of 2-KLG to ascorbic acid.

However, at the moment, the Reichstein process remains the method of choice due to the cheap availability of the starting substrate (glucose) and the chemical stability of the intermediates. The major disadvantage of the Reichstein process is the low percentage conversion from glucose. With process improvements made over the years, mainly in catalyst selections for the chemical steps and microorganism selection for the biostep, the current practical yield of the Reichstein process is still around 50%. Theoretically, one molecule of D-glucose can be converted to one molecule of L-ascorbic acid. However, due to specific molecular rearrangements, three hydrogen atoms and

from one to four oxygen atoms can not come from the D-glucose molecule. The theoretical yield is thus at best 87% (Boudrant, 1990).

This relatively low yield has led to a great deal of research in the past two decades into the possibility of bacterial fermentation processes capable of producing ascorbic acid. However, this is not the only reason. As public expectations for continuous progress towards achieving environmental sustainability continues to be strong, industries are driven to seek out green technologies. Adoption of these green technologies will still depend heavily upon "cost reduction." A replacement of the Reichstein process with a bacterial fermentation will ensure the lack of use of the various organic solvents and emissions of toxic pollutants that has become so ubiquitously associated with a chemical process. With the fast paced innovations in genetic engineering, many traditionally multi-stepped reactions may be realized in a single bacterial fermentation unit, thus saving capital spending.

1.2 Bacterial Bioprocesses for Ascorbic Acid Synthesis

At present, there are six bacterial fermentation processes for ascorbic acid production, all yielding 2-KLG as a direct precursor of ascorbic acid. The first pathway is the sorbitol pathway. Described for the first time by Motizuki in 1986 (Boudrant, 1990), sorbitol is transformed by fermentation to 2-KLG in a single staged bioreactor. The fermentation is performed by several *Pseudomonas* and *Acetobacter* strains, and the biochemical steps are unclear. The overall yield of this process does not exceed 10%, making this process unfit for commercialization. (Boudrant, 1990) The second pathway is the L-idonate pathway. The actual known intermediates are gluconate, 5-keto-D-

gluconate (5-KDG), L-idonate, and 2-keto-L-idonate. The first step involves an oxidation of gluconate to 5-KDG. Uses of various *Acetobacter*, *Pseudomonas*, and *Bacterium* strains are reported. The overall yield of the first step is about 90%. The second step is the reduction of 5-KDG to L-idonate. A *Fusarium* strain has been reported to yield an efficiency of 80%. (Sonoyama, 1982) The reaction is not direct and there is a loss of efficiency due to the reversion of 5-KDG to gluconate. The final step is the oxidation of L-idonate to yield 2-KDG. Various *Pseudomonas* and *Acetobacter*, *Cyanococcus*, and *Micrococcus* have been reported to yield an 80-90% conversion. Using three unique microorganisms, the overall yield of this process can reach 65% (Crawford, 1980).

The third pathway is the L-gulonate pathway, and it shares the first two steps with the L-idonate pathway. But the last reaction leads to the formation of L-gulonate, the precursor to 2-keto-L-idonate. A *Xanthomonas* strain has been reported with an efficiency of 90%. (Boudrant, 1990) The fourth pathway is the 2-KDG pathway, and it consists of three steps. The first is the oxidation of gluconate to 2-keto-D-gluconate (2-KDG). Various *Acetobacter*, *Pseudomonas*, and *Erwinia* strains have been reported. The second step is the oxidation of 2-KDG to 2,5-diketo-D-gluconate (2,5-DKG). These two steps have been reported to have a yield of 80%. The last step involves the reduction of 2,5-DKG to 2-KLG. This appears to be the rate-limiting step, with yields reported not exceeding 15%. However, present day performances using *Corynebacterium* are reported to be near 80%. Using three strains to carry out this transformation, the overall yield cannot exceed 65% (Kulahenek, 1970).

The fifth pathway is the 2,5-DKG pathway. This pathway allows the production of 2,5-DKG in a single step. The genus *Erwinia* is noted for this transformation. (Crawford, 1980) Given a glucose concentration of 200 g/L and fermentation time of 20 hours, the yield is about 75%. Moreover, fermentation using *Acetobacter cerenus* yields about 90% conversion (Sonoyama, 1987).

The final pathway is the 2-KLG pathway. This direct pathway from glucose to 2-KLG has been made possible only in the recent years with new emerging technology: mixed cultures, mutant selection, isolation of 2,5-DKG reductase in *Corynebacterium*, and gene transfer of in *Corynebacterium* into *Erwinia* or *Acetobacter*. (Lazarus, 1990) Using a mixed culture, yields have reached about 90%. However, with the aid of genetic engineering techniques, this pathway can be performed in a single step with a much lower performance of approximately 30% (Boudrant, 1990).

Of the six bacterial fermentation processes, the sorbitol pathway is clearly inferior due to its low yield of 20%. The idonic, gulonic acid, and 2-KDG pathways offer only slight improvements to the Reichstein process in terms of overall yield. The 2-KLG direct synthesis pathway is the most innovative; however, there are many genetic engineering issued to be worked out. Such issues include the low yield of 2,5-DKG reductase, facility of 2,5-DKG and 2-KLG transport across the cellular membrane, and the regeneration of NADPH to meet necessary reducing power. The pathway that offers the most promising possibilities currently is the 2,5-DKG pathway. Sonoyama has already demonstrated a 90% conversion rate in a dual-staged fermentation system.

All of these possible replacement pathways for the Reichstein process utilize whole cells in batch fermentors with glucose as a substrate. Thus far, no research has been focused on the possibility of a nonviable cell system. The advantages of such a system include theoretical higher conversions compared to the whole cells. This is so because glucose uptake into central metabolism is eliminated. Any glucose diverted to the central metabolism pathway in a whole cell system may be converted to product in a nonviable cell system.

1.3 Purpose

The purposes of this research was to (a) determine the degree to which central metabolism effects glucose utilization in the batch production of 2,5-DKG in both viable and nonviable *P. citrea* cells, (b) develop a mathematical model for 2,5-DKG batch production that accounts for glucose utilization by the enzymes responsible for 2,5-DKG production and by central metabolism, and (c) validate the mathematical model by applying it to various cases of batch production using both viable and nonviable cells.

2 Objectives

The objectives of this research were to study the degree to which central metabolism effects glucose utilization in the batch production of 2,5-DKG and to develop and validate a mathematical model based on the key components of the bacteria *P. citrea* to describe the batch production of 2,5-DKG. These objectives were addressed in the following tasks:

- Determination of the growth rates of *P. citrea* on various carbohydrate substrates
- Determination of the activity of the enzymes representing major pathways for glucose degradation in *P. citrea* cells during both log growth and stationary phases
- Determination of the role central metabolism plays in batch production of 2,5-DKG by utilizing both viable and nonviable *P. citrea* cells in production
- Development of a mathematical model describing the batch production of 2,5-DKG by incorporating the Michaelis-Menten enzyme kinetics of the enzymes involved in the production of 2,5-DKG in *P. citrea*
- Validation of the model developed with batch 2,5-DKG production data

3 Literature Review

3.1 Overview

In this study, four possible routes for the utilization of glucose by P. citrea cells were considered: 1) the Embden-Meyerhof-Parnas (EMP) pathway, 2) the Entner-Douderoff (ED) pathway, 3) the pentose phosphate pathway, and 4) the extracellular degradation of glucose via a three enzyme system to form 2,5-DKG. Of these four possible pathways, the first three are part of the cells' central metabolism and are thus undesirable in the production of 2,5-DKG since they channel the substrate glucose away from the formation of the product 2,5-DKG. Each of the three pathways associated with central metabolism involve several enzymes and parts of each pathway share the same enzymes (see Figure 3-1). Therefore, in order to determine the relative activity of the various pathways, it is necessary to identify the enzyme(s) which are unique to each pathway. After these enzymes (hereafter referred to as the "key" enzyme(s) of the corresponding pathway) are identified, the enzymatic activity may be assayed to determine the relative activities of the associated pathway. For the pathways associated with central metabolism, Section 3.1 describes each pathway in detail and identifies the key enzyme(s) of each pathway. Section 3.2 describes the details of the three enzyme system responsible for the extracellular degradation of glucose to form 2,5-DKG. Sections 3.3 - 3.5 discuss the techniques by which the kinetics of the enzymes are quantified.

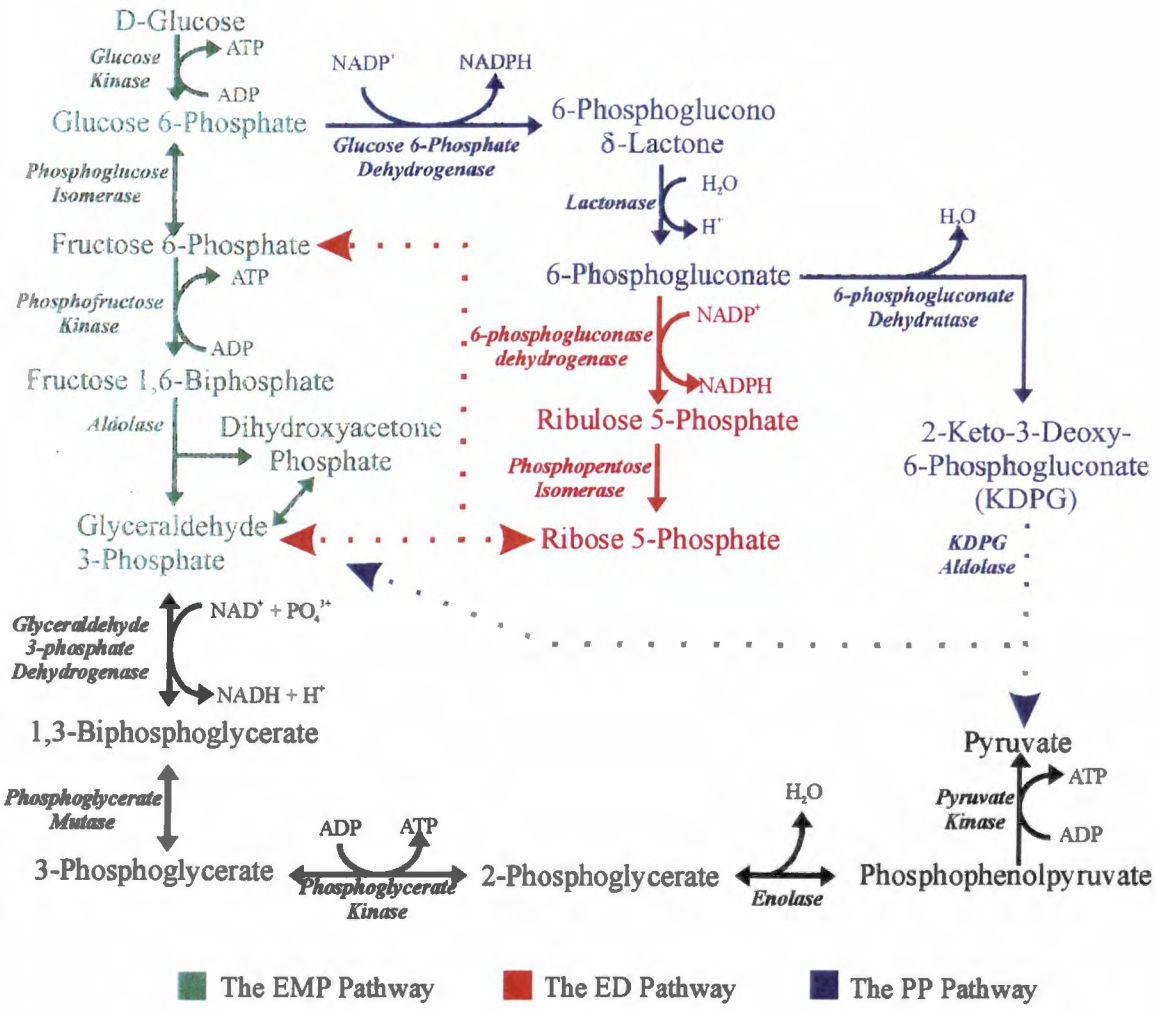


Figure 3-1 Glucose utilization pathways associated with cellular central metabolism

3.2 Central Metabolism

In order to survive and prosper, bacteria have to extract energy and reducing power from their environment and to synthesize the building blocks for their macromolecules. These two objectives are executed by a highly integrated network of chemical reactions. It is this complex network that has come to be called cellular metabolism. By extracting energy from the environment, bacteria are able to grow with a number of substrates in the presence of oxygen or in its absence. Under aerobic conditions part of the substrate is oxidized to CO_2 with oxygen as the terminal electron acceptor. However, electrons are not transferred directly from the fuel molecules and their oxidized forms to oxygen. Instead, these substrate transfer electrons to special carriers which are either pyridine nucleotides or flavins. These high potential electrons derived from the oxidation of fuel molecules can either be utilized in ATP production via oxidative phosphorylation or in biosynthesis which require reducing power in addition to ATP because in most biosynthesis, the precursors are more oxidized than the products. (Lehninger, 1982) Nicotinamide adenine dinucleotide (NAD^+) is a major electron acceptor in the oxidation of fuel molecules. The reduced form of this carrier is NADH. The electron donor in most reductive biosynthesis is NADPH, the reduced form of nicotinamide adenine dinucleotide phosphate ($NADP^+$). These two electron carriers are very similar in structure and share the same mechanism for carrying electrons. However, NADPH is used almost exclusively for reductive biosynthesis, whereas NADH is used primarily for the generation of ATP (Stryer, 1995).

The fuel molecules thus serve two purposes. The first purpose is the production of ATP, and the EMP pathway converts glucose into pyruvate coupled with a relatively small amount of ATP. The second purpose is to generate the reducing power needed for biosynthesis in the form of NADPH. The pentose phosphate pathway is responsible for converting glucose into various intermediates needed for biosynthesis purposes coupled with the generation of reducing power, NADPH. Roughly 50% conversion of a substrate, such as glucose, will result in enough ATP production to convert the other 50% into cell material. (Gottschalk, 1986) In order to utilize the energy released during glucose oxidation to CO_2 for the purpose of ATP generation, glucose must undergo a series of reaction, which may seem at first overwhelming, but upon close scrutiny, coherent and economical patterns emerge.

3.2.1 Glucose Transport

The cellular membrane of *E. coli*, notably the most studied bacteria, is not simply permeable to glucose. There is no simple diffusion of glucose in and out of the bacterial cells which would allow equal intracellular and extra-cellular concentrations of glucose. Instead, *E. coli* possesses a system that is specific for glucose transport. This transport process "picks up" glucose at the medium side of the membrane and releases it on the cytosol side of the membrane. This transport process is coupled to a chemical conversion of the substrate - the phosphorylation of glucose to glucose 6-phosphate. The phosphate donor in this reaction is phosphoenolpyruvate and the enzyme complex catalyzing this transport process is the glucose phototransferase system (Gottschalk, 1986).

To synthesize ATP, glucose 6-phosphate passes through the Embden-Meyerhof-Parnas pathway and is oxidized to form pyruvate. Pyruvate is further oxidized to acetyl-coenzyme A and enters the tricarboxylic acid (TCA) cycle. The acetyl part of the acetyl-coenzyme A is further oxidized to CO_2 in the TCA cycle in turn generating reducing power in the form of various reduced coenzymes. These reduced coenzymes are further oxidized in the repiratory chain, which is coupled with mechanisms for ATP synthesis.

3.2.2 The Embden-Meyerhof-Parnas (EMP) Pathway

The EMP pathway is the most commonly used set of reactions for the conversion of glucose to pyruvate, and is a major pathway for glucose degradation. Not only are two pyruvate molecules formed through this pathway per molecule of glucose, 2 ATP and NADH molecules are also formed. The purpose of the EMP pathway is not only to degrade glucose in order to generate ATP, but also to provide building blocks, intermediates and reducing powers, for other pathways, such as fatty acid synthesis, and the TCA cycle (Stryer, 1995).

The key enzyme for the EMP pathway is phosphofructokinase because it is unique to this pathway. Phosphofructokinase catalyzes the transfer of a phosphate group from ATP to phosphorylate fructose 6-phosphate in the 1 position to yield fructose 1,6-diphosphate. Mg^{2+} is required for this essentially irreversible reaction. Phosphofructokinase is the key enzyme in the control of the EMP pathway, and is activated by a low concentration of ATP and inhibited by a high concentration of ATP (Lehninger, 1982).

3.2.3 The Entner-Douderoff (ED) Pathway

Besides the EMP pathway, there is a second important pathway used for glucose catabolism. Widely found in bacteria, the ED pathway is first discovered in *Pseudomonas saccharophilas*. The ED pathway is very similar to the EMP pathway, differing only in the byproducts formed. Only 1 molecule of ATP, NADH, and NADPH each is formed per molecule of glucose entering the pathway, compared with 2 molecules of ATP and NADH formed in the EMP pathway. One of the purposes of the ED pathway is to breakdown glucose in bacteria lacking phosphofructokinase, thus unable to utilize the EMP pathway. The ED pathway is also important when compounds such as gluconate, mannonate, or hexuronates serve as substrates. Clearly, the EMP pathway is not very useful when it comes to breaking down gluconate. The ED pathway is fairly widespread, particularly among Gram-negative bacteria, while it is not very common in anaerobes. Anaerobes lack a respiratory chain and must gain their ATP by substrate level phosphorylation. The EMP pathway is more efficient because it produces 1 additional ATP for every 2 pyruvates than the ED pathway (Gottschalk, 1986).

The key enzymes in the ED pathway are 6-phosphogluconate dehydratase and 2-keto-3-deoxy-6-phosphogluconate aldolase. 6-phosphogluconate dehydratase catalyzes the dehydration reaction of gluconate 6-phosphate to form 2-keto-3-deoxy-6-phosphogluconate (KDPG). KDPG aldolase catalyzes the aldol cleavage of KDPG to form pyruvate and 3-phosphoglyceraldehyde. The ED pathway can be distinguished by the presence of these two enzymes. If high levels of the 6-phosphogluconate dehydratase

and KDPG aldolase exist, it is likely that the ED pathway is involved in glucose degradation (Gottschalk, 1986).

3.2.4 The Pentose Phosphate (PP) Pathway

Glucose is not only utilized by the bacteria to make ATP but also to make building block precursors of cell macromolecules. The PP pathway provides an alternate route for glucose degradation. It traces the conversion of glucose to pentose phosphates, which act as precursors to the ribose and deoxyribose in nucleic acids. From 1 molecule of glucose entering the pathway, 1 molecule is ribose 5-phosphate is formed along with 2 molecules of NADPH. The ribose 6-phosphate may either be further converted to phospho-glyceraldehyde and enter the EMP pathway or enter other biosynthetic pathways. The primary purposes of the pentose phosphate pathway is to generate not only reducing power, in the form of NADPH, needed in biosynthesis but also intermediates for other pathways. The key enzyme for the PP pathway is 6-phosphogluconate dehydrogenase because it is unique to this pathway, and easily identifiable (Lehninger, 1982).

3.3 Extracellular Degradation of Glucose

In addition to the intracellular central metabolic pathways, glucose may also be degraded via gluconate externally on the medium side of the cell membrane. This is shown in a number of *Pseudomonads*. A glucose dehydrogenase, bound to the membrane, converts glucose to gluconate. The latter may be phosphorylated to gluconate 6-phosphate and enter the cell or be further oxidized to 2-KDG. Glucose and gluconate

dehydrogenases are membrane-bound and feed electrons directly into the respiratory chain. These enzymes are significant in the evolution sense because they allow the extracellular conversion of glucose into substrates less utilizable by other microbes than glucose. Thus these enzymes benefit the *Pseudomonads*, which can in turn transport and degrade glucose, gluconate, and 2-ketogluconate (Gottschalk, 1986).

3.3.1 Bioconversion of Glucose to 2,5-DKG

In addition to *Pseudomonads*, several species of the genera *Acetobactor*, *Gluconobacter*, and *Erwinia* are known to degrade glucose externally. Figure shows the oxidation of glucose by these ketogenic bacteria to gluconate, 2-KDG, and finally 2,5-DKG. This oxidation of glucose to ketogluconates in a wide variety of ketogenic bacteria has been shown to proceed via membrane-bound dehydrogenase enzymes that are linked to the electron transport chain. Subsequent reduction of the ketogluconates or their phosphorylated forms is catalyzed by NADP(H) linked reductases in the cytosol. The products of these reactions can then enter into central metabolism.

The carbohydrate oxidizing enzymes are found to be membrane-bound dehydrogenases based on the following observations (Lazarus, 1990):

- the activities are found in the membrane fraction obtained by ultracentrifugation
- the activities are solubilized by a variety of detergents
- artificial electron acceptors such as ferriccyanide or 2,6-dichloro-indophenol are reduced in place of O_2 as electron acceptor.

Thus evidence for glucose dehydrogenase, gluconate dehydrogenase, 2-ketogluconate dehydrogenase has been observed. These enzymes are most likely heme and flavin containing proteins linked to the cytochrome chain (Ameyama, 1978).

3.3.2 Glucose Dehydrogenase

Glucose dehydrogenase catalyzes the oxidation of glucose to a gluconolactone. The solubilized glucose dehydrogenase isolated from *Pseudomonas aeruginosa* appears to be monomeric in the presence of 1% Triton X-100. The enzyme appears to be a single peptide with a molecular weight of about 90 KDa. The enzyme reacts with various artificial electron acceptors such as phenazine methosulfate, 2,6-dichloro-phenolindophenol, and ferricyanide. The enzyme has a dual optimum pH depending on the electron acceptor. With ferricyanide, the optimal pH is more acidic. The enzyme possesses fairly broad substrate specificity, and the reaction product is a gluconolactone, which can in turn be converted to gluconate via a spontaneous hydrolysis (Ameyama, 1981).

3.3.3 Gluconate Dehydrogenase

Gluconate dehydrogenase catalyzes the oxidation of gluconate to 2-KDG. The solubilized enzyme from *Pseudomonas aeruginosa* is a monomer in the presence of at least 1% Triton X-100. Removal of Triton X-100 causes the enzyme to become dimeric, in turn decreasing the activity. In the presence of sodium dodecyl sulfate, the enzyme dissociates into three components. Two of those components consist of a flavoprotein and a cytochrome c_1. The third component remains a mystery. Gluconate is oxidized in

the presence of ferricyanide and other artificial agents, such as phenazine methosulfate and 2,6-dichlorophenolindophenol. NAD and NADP do not function as electron acceptors. (Matsushita, 1980)

3.3.4 2-KDG Dehydrogenase

2-KDG dehydrogenase catalyzes the reaction of 2-KDG to 2,5-DKG. Solubilization and purification of 2-KDG dehydrogenase from the membrane fraction of *Gluconobacter melanogenus* resulted in a 400-fold purity yield of 41%. The purified enzyme is a dehydrogenase-cytochrome complex tightly bound to a c-type cytochrome. The molecular weight was determined to be about 133,000 Daltons. Like gluconate dehydrogenase, 2-keto-D-gluconate dehydrogenase dissociates into three parts in the presence of sodium dodecyl sulfate: a flavoprotein, a cytochrome, and a mystery component. The dehydrogenase is found to be a flavoprotein having a covalently bound flavin. 2-keto-D-gluconate is oxidized only in the presence of dyes, such as ferricyanide, phenazine methosulfate or 2,6-dichlorophenolindophenol. NAD and NADP do not function as electron acceptors (Shinagawa, 1981).

3.4 Summary of Glucose Metabolic Pathways in *P. citrea*

The four pathways for glucose metabolism in *P. citrea* are summarized in Figure 3-2. The internal pathways are the EMP, ED, and PP pathways. The extracellular pathway is the 2,5-DKG pathway. Each pathway is distinguished by the key enzyme associated with that pathway. The activity of each of the key enzyme is representative of the activity of that pathway in glucose metabolism. The major pathways for glucose

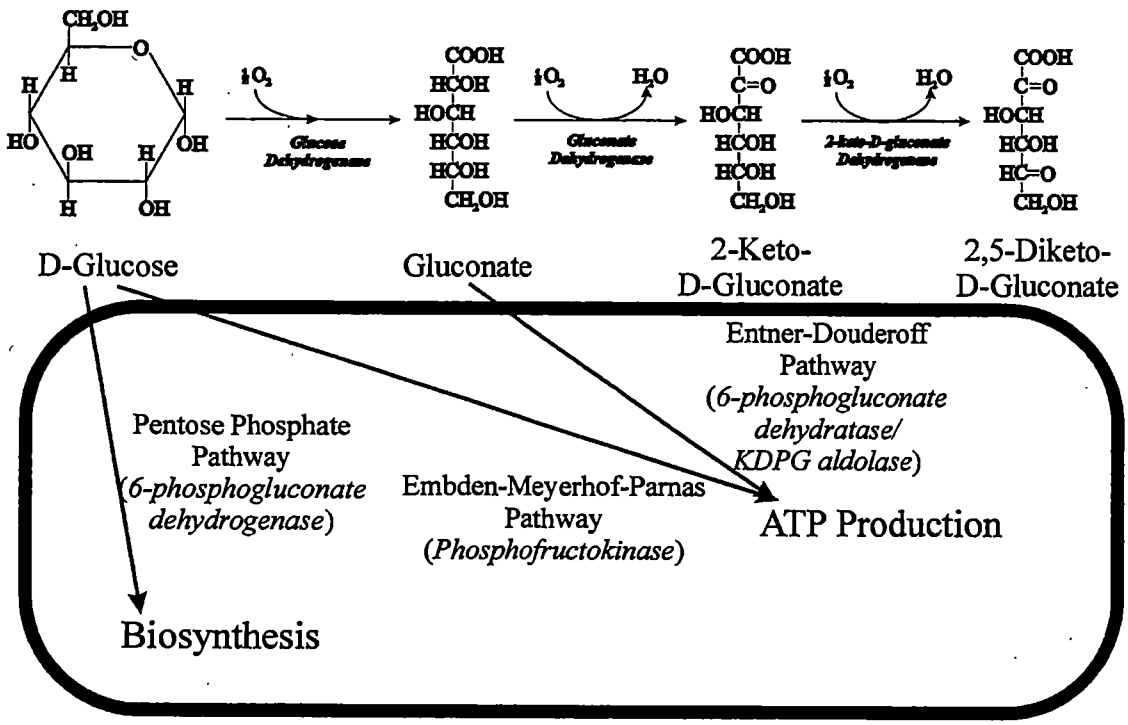


Figure 3-2 Summary of major pathways of glucose metabolism and the key enzyme(s) involved in each pathway

degradation and the associated key enzyme(s) are listed in Table 3-1. The external pathway for glucose metabolism which produces 2,5-DKG is in italics.

Table 3-1 Major pathways and associated key enzyme(s) for glucose metabolism

Pathway Considered	Key Enzyme(s)
Embden-Meyerhof-Parnas (EMP) pathway	Phosphofructokinase
Entner-Douderoff (ED) pathway	6-phosphogluconate dehydratase / KDPG aldolase
Pentose Phosphate (PP) pathway	6-phosphogluconate dehydrogenase
2,5-DKG pathway	*2-KDG dehydrogenase*

3.5 Enzyme Mechanisms

Enzymes are highly specialized proteins with catalytic activity. The extraordinary catalytic powers exhibited by enzymes exceed by far that of synthetic catalysts. Enzymes have a high degree of specificity for their substrates, accelerate reactions without formation of byproducts, function in dilute aqueous solutions under very mild conditions of pH and temperatures. Few nonbiological catalysts show all these characteristics. All pure enzymes examined to date are proteins; more over, their catalytic activities depend upon the integrity of their structures as proteins. Enzymes are usually high in molecular weight, like most proteins. Thus, they are very large compared with the substrates or the function groups. Enzymes may be simple in structure, such as a folded polypeptide chain, or be comprised of more than one sub-unit. Furthermore, the enzyme activity may be attributed to the activation by a non-protein group. Such groups are known as cofactors, such as NAD(P), CoA, and ferricyanide. Because of an enzyme's high

specificity for the substrate and cofactors, two molecules serving the same function may not work for the same enzyme (Stryer, 1995).

Enzymes are true catalysts in that they enhance the rate of specific chemical reactions that would otherwise occur only very slowly. They cannot change the equilibrium point of the reactions they promote, nor are they used up or permanently change by these reactions. Enzymes enhance the rate of chemical reactions by lowering the activation energy. This is achieved when the enzyme binds to the substrate and forms an enzyme-substrate complex. The molecular aspects of this phenomenon are not yet fully understood. The substrate binds to a specific site on the enzyme known as the active site. In a reaction involving more than one substrate, enzymes can hold substrates such that reactive regions of substrates are close to each other and to the enzyme's active site, which is known as the proximity effect. Also, enzymes may hold the substrates at certain positions and angles to improve the reaction rate, which is known as the orientation effect. The reaction rate is greatly affected by the conformation of the enzyme itself (Lehninger, 1982).

3.6 Michaelis-Menten Enzyme Kinetics

Many enzymes show the typical hyperbolic curve (see Figure 3-3) relating the reaction velocity to the substrate concentrations, with the gradual approach to saturation of the enzyme with substrate. By following either the rate of substrate consumption or the rate of formation of reaction products, several similarities on the measured rates of enzymatic reactions were witnessed. The rate of reaction is first order in substrate concentration at relatively low substrate concentrations. As substrate concentration

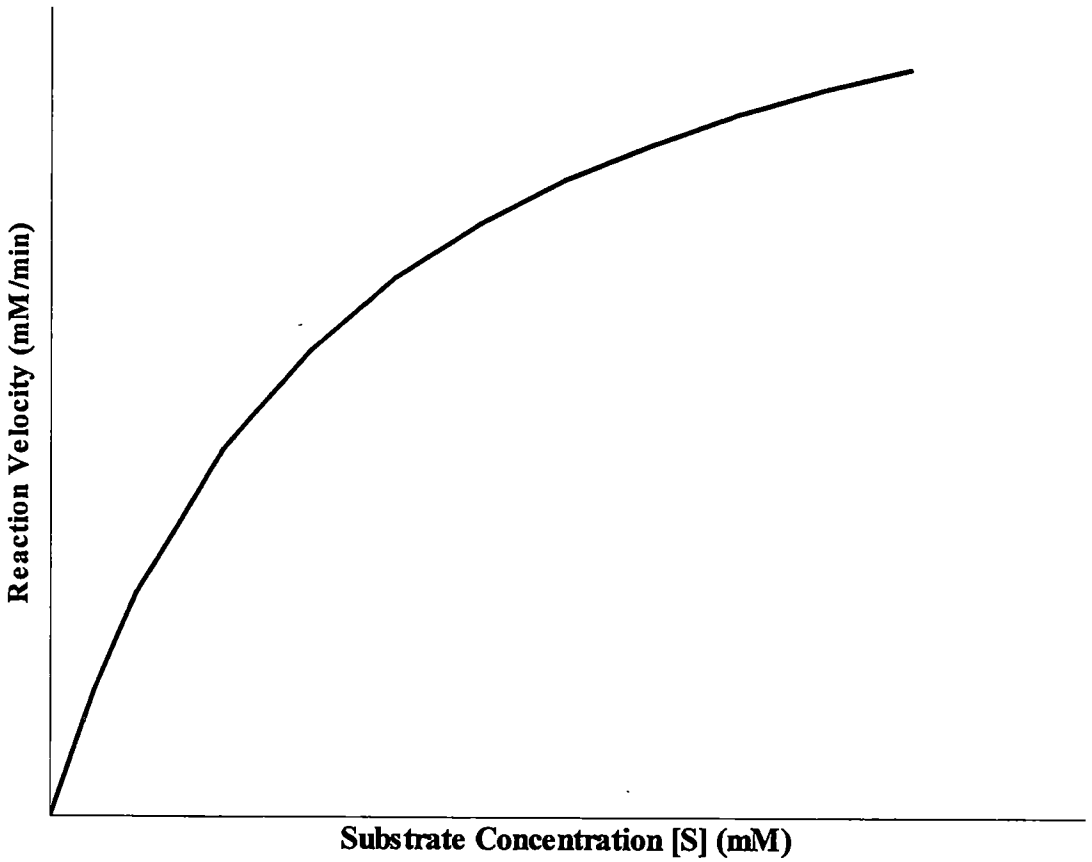


Figure 3-3 A plot of the reaction velocity as a function of the substrate concentration [S] for an enzyme obeying Michaelis-Menten kinetics

increases, the rate of reaction decreases to zero for the substrate. The rate of reaction is proportional to the enzyme concentration (Lehninger, 1982).

A mathematical model of the kinetics of a single substrate enzyme-catalyzed reaction was first developed by V.C.R. Henri in 1902 and by L. Michaelis and M. Menten in 1913. An enzyme solution has a fixed number of active sites to which substrates can bind. At high substrate concentrations, all these sites may be occupied by substrates or the enzyme is saturated. Saturation kinetics may be obtained from a simple reaction scheme that involves a reversible step for enzyme-substrate complex formation and a dissociation step of the enzyme-substrate complex.

$$E + S \underset{k_{-1}}{\overset{k_1}{\longleftrightarrow}} ES \xrightarrow{k_2} E + P \qquad \textbf{3-1}$$

where E = enzyme
S = substrate
ES = enzyme-substrate complex
P = product
k_1 = rate constant of the forward reaction in the first step
k_{-1} = rate constant for the reverse reaction in the second step
k_2 = rate constant for the forward reaction in the second step

It is assumed that the ES complex is established rather rapidly and the rate of the reverse reaction of the second step is negligible. The assumption of an irreversible second reaction often holds only when product accumulation is negligible at the beginning of the reaction. In deriving the final expression of the Michaelis-Menten equation, an algebraic description of the hyperbolic curve of the saturation kinetics, it is assumed that the reaction involved in the first step is in steady state. Starting with a

concentration of unreacted catalyst, E_t, the rate of formation of ES equals the rate of breakdown of ES:

$$\text{Rate of formation of ES} = k_1([E_t]-[ES])[S] \qquad \textbf{3-2}$$

$$\text{Rate of breakdown of ES} = k_{-1}[ES]+k_2[ES] \qquad \textbf{3-3}$$

A mass balance on the enzyme yields:

$$[E]+[ES]=[E_t] \qquad \textbf{3-4}$$

The reaction velocity V_0 is equal to the rate of breakdown of the ES complex:

$$V_0 = \frac{d[P]}{dt} = k_2[ES] \qquad \textbf{3-5}$$

These equations may be combined with the assumption that the rate of formation of ES equals the rate of breakdown of ES to yield the final expression for the Michaelis Menten equation:

$$V_0 = \frac{V_{\max}[S]}{K_m+[S]} \qquad \textbf{3-6}$$

Where $V_{\max} = k_2[E_t]$ and $K_m = \frac{k_2+k_{-1}}{k_1}$

At low substrate concentrations, when [S] is much smaller than K_m, the velocity is directly proportional to substrate concentration, with a proportionality constant of V_{max}/K_m. At high concentrations, when [S] is much larger than K_m, the velocity becomes V_{max}. The rate becomes maximal and is independent of the substrate concentration.

3.7 Lineweaver-Burk Plots

The Michaelis-Menten constants V_{max} and K_m may be readily derived from rates of catalysis measured at different substrate concentrations. The Michaelis Menten equation (Equation 3-6) may be transformed into other forms that are more useful in plotting experimental data. One common transformation is derived by simply taking the reciprocal of both sides of the Michaelis-Menten equation to give:

$$\frac{1}{V_0} = \frac{K_m + [S]}{V_{max}[S]} \qquad \textbf{3-7}$$

Equation 3-7 may be further simplified by separating the components in the numerator and canceling out similar terms in the numerator and denominator to give:

$$\frac{1}{V_0} = \frac{K_M}{V_{max}} \frac{1}{[S]} + \frac{1}{V_{max}} \qquad \textbf{3-8}$$

Equation 3-8 is a transformation of the Michaelis-Menten equation known as the Lineweaver-Burk equation. For enzymes obeying the Michaelis-Menten relationship, a plot of $1/V_0$ against $1/[S]$ yields a straight line. This line will have a slope of K_m/V_{max} and a y-intercept of $1/V_{max}$. The Lineweaver-Burk plot has the great advantage of allowing more accurate determination of V_{max}, which can be approximated from a simple plot of V_0 vs. [S] plot.

4 Materials and Methods

4.1 Materials

Pantoea citrea ATCC 39140, formerly *Acetobacter cerinus*, was obtained from the American Type Culture Collection (ATCC, Rockville, MD). *Escherichia coli* DH5α was a generous gift from Dr. Anthony Hay (Center for Environmental Biotechnology, The University of Tennessee, Knoxville, TN). Glucose dehydrogenase isolated from *Bacillus megaterium*, gluconate dehydrogenase from *Pseudomonas sp.*, aldolase, α-glycerolphosphate dehydrogenase and triosephosphate isomerase from rabbit muscles were all purchased from Sigma (St. Louis, MO). 2,5-DKG standards were generously provided by Genecor International (Santa Palo, CA).

4.2 Frozen Stock Preparation

The freeze-dried *P. citrea* obtained from ATCC was rehydrated in a 250-ml shake flask with 100 ml of growth medium (pH=6.5) consisting of 6 g/L monobasic potassium phosphate, 4 g/L dibasic potassium phosphate, 1 g/L glutamic acid, 1 g/L magnesium sulfate, 1 g/L yeast extract, and 5 g/L glucose. This mixture was placed in a New Brunswick rotary shaker (Edison, NJ) overnight at 300 RPM and 28 °C. Optical density of this culture was monitored by measuring absorbance at 600 nm in a Beckman DU60 spectrophotometer (Fullerton, CA). Once the overnight mixture reached an optical density of 1.2, the frozen cell stock mixture consisting of 50% overnight mixture and 50% glycerol was prepared and stored at -80 C in aliquots of 1 ml.

4.3 Preparation of Cell Free Extract for Intracellular Enzyme Assays

One ml of the frozen *P. citrea* was innoculated into a 250-ml shake flask with 100 ml of growth medium (pH=6.5) consisting of 6 g/L monobasic potassium phosphate, 4 g/L dibasic potassium phosphate, 1 g/L glutamic acid, 1 g/L magnesium sulfate, 1 g/L yeast extract, and 5 g/L carbon source. For studies using cells in log growth phase, the carbon sources used were glucose, fructose, gluconate, and pyruvate. For studies using cells in stationary phase, only glucose was used as the carbon source. This culture mixture was placed in a New Brunswick rotary shaker (Edison, NJ) overnight at 300 RPM and 28 °C until the absorbance reading at 600 nm was about 1.2. Cells from this overnight culture were then used to prepare cells in either log growth phase or stationary phase.

To prepare the cells in log growth phase, approximately 5 ml of the overnight culture was innoculated into 250 mL flasks containing 100 mL of fresh growth medium (keeping the carbon source used constant; for example, 5 ml of overnight culture grown on glucose were innoculated into 100 ml of fresh growth medium containing glucose as the sole carbon source). The new culture was placed in the rotary shaker at 300 RPM and 28 °C. After 5 hours, the contents of the flask (broth containing cells in log growth phase) were harvested.

To prepare the cells in stationary phase, all of the overnight culture was used to inoculate a bioreactor with 2 L of final growth medium. The 2-L final growth medium consisted of two parts. The 1.8-L autoclavable portion consisted of: 18.4 g KH_2PO_4, 3.2 g $MgSO_4 \bullet 7H_2O$, 18.8 g $(NH_4)_2SO_4$, 30 g glutamic acid, and 0.224 g choline chloride in 1.6

L of water. The remaining 0.4-L portion consisted of 48.43 g fructose, 66.87 g glucose, and 33.4 mg nicotinic acid in 200 ml of water and was sterilized by filtration using a filter with 0.2 micron pore size. The rotational agitation speed was held constant at 1000 RPM. Temperature was held constant at 28 °C. The pH was controlled at 5.8 using 2 M KOH. Air was fed in at 2.5 L/min. Cells were grown for 12-15 hours until a sharp increase in % dissolved oxygen was observed (shown in Figure 4-1), indicating that the cells were in stationary phase. At hour intervals for five hours, 5 ml of reactor broth were harvested.

After harvesting, the cell broth was centrifuged at 10,000 RPM for 25 min with a Beckman J2-21 (Fullerton, CA) centrifuge. In order to wash the cells, the cell pellet was resuspended with tris-HCl buffer (pH=6.5) consisting of 0.05 M tris-HCl, and 1 mM EDTA (sodium salt). The mixture was again centrifuged, and the supernatent was discarded. This wash step was repeated. The cell pellet was finally resuspended in 2 ml of the same buffer. The resuspended cell mixture was then sonically disrupted using a sonicator (Virtus Corp., Gardiner, NY) in three 30 second treatments with intermittent cooling on ice. The sonically treated mixture was then ultracetrifuged in a Beckman L8-80M ultracentrifuge for 1 hour at 21000 RPM. The supernatant was retained as the crude enzyme extract and used for intracellular enzyme assays.

4.4 Intracellular Enzyme Assays

All intracellular enzyme assays involved the disappearance of reduced nicotiamide dinucleotide (NADH) or the appearance of reduced NADP (NADPH), which may be monitored by measuring changes in the absorbance of the assay mixture at 340

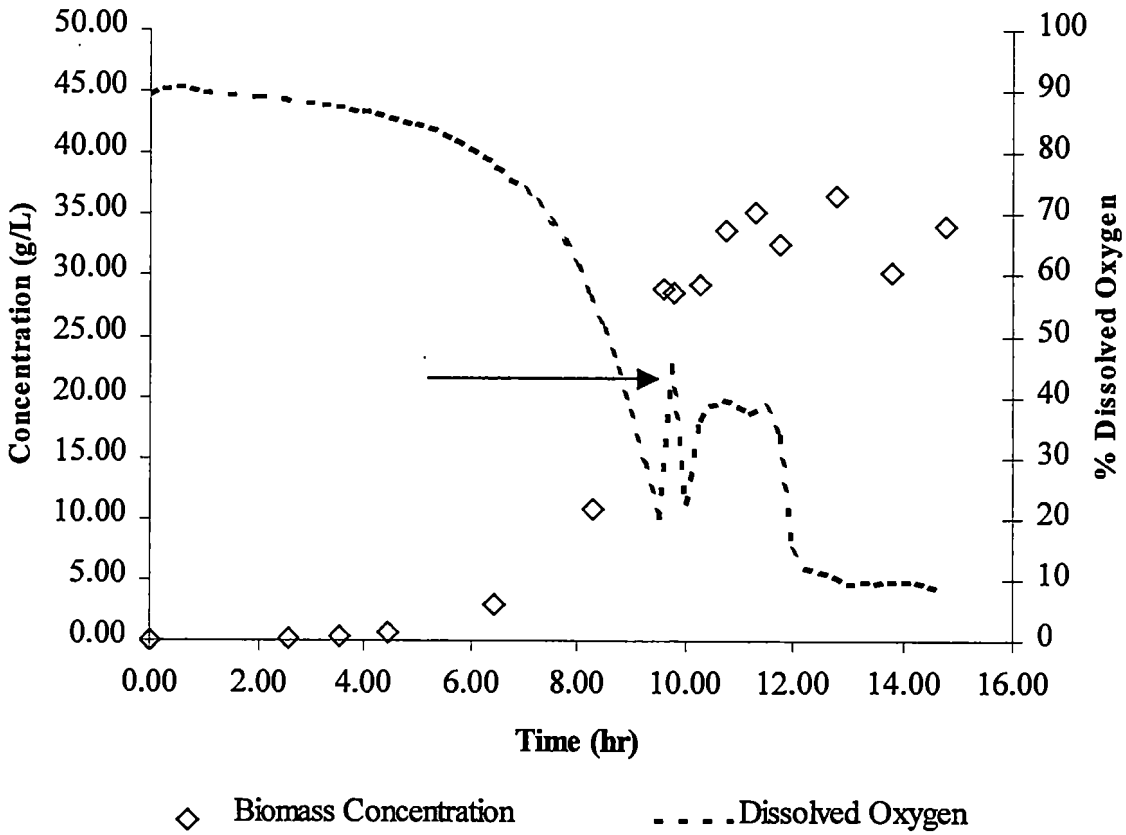


Figure 4-1 The sharp rise (indicated by the arrow) in % dissolved oxygen after 10 hours of growth, indicating the beginning of stationary phase

nm with a spectrophotometer. The absorbance measurements were converted to nanomoles of NADPH formed or NADH consumed per minute per milligram of protein, assuming a molar extinction coefficient of 6220 M^{-1} for NADPH and NADH (Gerhardt, 1994). All assays were carried out in a 1-ml cuvette at room temperature. The cuvette was placed in the spectrophotometer, and the reaction was started upon the addition of the active substrate. Upon the start of the reaction, readings were taken at 30-second intervals for 3 minutes. Experiments using control samples were performed to monitor the natural decay in absorbance of NADH degradation and natural increase of absorbance of NADPH formation.

4.4.1 6-Phosphoglyconate Dehydrogenase

As discussed previously, 6-phosphogluconate dehydrogenase is the key enzyme of the PP pathway, catalyzing the oxidation of 6-phosphogluconate to 5-phosphoribulose and CO_2. The enzyme may be assayed by monitoring the formation of NADPH coupled with the oxidation of 6-phosphogluconate (Rippa, 1975). The overall reaction is shown in Equation 4-1:

$$\text{6-phsphogluconate} + \text{NADP} \rightarrow \text{ribulose 5-phosphate} + CO_2 + \text{NADPH} + H^+ \qquad \textbf{4-1}$$

One milliliter of reaction mixture contained: 0.1 ml of 0.015M NADP, 0.1 ml of the crude enzyme extract, 0.7 ml of 0.05M tris-HCl with 1 mM EDTA, and 0.1 ml of 0.05 M 6-phosphogluconate. One milliliter of the control mixture contained: 0.1 ml of 0.015M NADP, 0.1 ml of the crude enzyme extract, 0.8 ml of 0.05M tris-HCl with 1 mM EDTA, and no 0.05 M 6-phosphogluconate. The reaction was started with the addition of

the NADP. A unit of enzyme was defined as that amount which catalyzes the formation of 1 μmole of NADPH per minute under the conditions above. The specific activity was expressed as units of enzyme per mg of intracellular protein.

4.4.2 6-Phosphogluconate dehydratase and KDPG aldolase

6-Phosphogluconate dehydratase and KDPG aldolase are the key enzymes of the ED pathway catalyzing the formation of pyruvate and 3-phosphoglyceraldehyde from 6-phosphogluconate. These two enzymes were assayed together by following the formation of pyruvate from 6-phosphogluconate. The pyruvate formed was then converted to lactate by excess rabbit muscle lactate dehydrogenase, and NADH disappearance was measured (Lessie, 1967). The overall reaction is shown in Equation 4-2:

$$\text{6-phosphogluconate} + \text{NADH} + \text{H}^+ \rightarrow \text{L-lactate} + \text{NAD}^+ + \text{3-phosphoglyceraldehyde} \qquad \textbf{4-2}$$

One milliliter of reaction mixture contained: 0.1 ml of 0.1M $MgCl_2$, 0.1 ml of 3 mM NADH, 0.1 ml of the crude enzyme extract, 0.1 mg of lactate dehydrogenase, 0.1 ml of 0.02M 6-phosphogluconate, and 0.6 ml of 0.05M tris-HCl with 1 mM EDTA. One milliliter of the control mixture contained: 0.1 ml of 0.1M $MgCl_2$, 0.1 ml of 3 mM NADH, 0.1 ml of the crude enzyme extract, 0.1 mg of lactate dehydrogenase, no 6-phosphogluconate, and 0.7 ml of 0.05M tris-HCl with 1 mM EDTA. The reaction was started by the addition of 6-phosphogluconate. A unit of enzyme was defined as that amount which catalyzes the oxidation of 1 μmole of NADH per minute under the

conditions above. The specific activity was expressed as units of enzyme per mg of intracellular protein.

4.4.3 Phosphofructokinase

Phosphofructokinase is the key enzyme of the EMP pathway, catalyzing the phosphorylation on the carbon 1 of fructose 6-phosphate to form fructose 1,6-diphosphate. The enzyme may be assayed by following the formation of fructose 1,6-diphosphate from fructose 6-phosphate. The fructose 1,6-diphosphate was then converted to α-glycerphosphate in the presence of aldolase, triosephosphate isomerase, α-glycerophosphate dehydrogenase, and NADH (Kemerer, 1975). The overall reaction is shown in Equation 4-3.

$$\text{ATP} + \text{fructose 6-phosphate} + \text{NADH} \rightarrow \text{ADP} + \alpha\text{-glycerolphosphate} + \text{NAD}^+ \qquad \textbf{4-3}$$

Aldolase and a mixture α-glycerophosphate dehydrogenase and triosephosphate isomerase were mixed with a buffer solution of 0.01 M tris-HCl and 0.002 M EDTA (pH=8) to yield a solution containing 1.5 mg/ml of aldolase and 0.5 mg/ml of α-glycerophosphate dehydrogenase and triosephosphate isomerase. The auxiliary enzyme mixture was dialyzed with the same buffer in a 1-L beaker at 4°C overnight. The dialyzing buffer was changed after 6 hours.

One ml of the reaction mixture contained: 0.1 ml of 0.01 M of $MgCl_2$, 0.1 ml of 1.5 mM NADH, 0.1 ml of the auxiliary enzyme mix, 0.1 ml of the crude enzyme extract, 0.4 ml of 0.05 M Tris-HCl with 1 mM EDTA, 0.1 ml of fructose 6-phosphate, and 0.1 ml

of 0.03 M ATP. One ml of the control mixture contained: 0.1 ml of 0.01 M of MgCl2, 0.1 ml of 1.5 mM NADH, 0.1 ml of the auxiliary enzyme mix, 0.1 ml of the crude enzyme extract, 0.5 ml of 0.05 M Tris-HCl with 1 mM EDTA, 0.1 ml of fructose 6-phosphate, and no ATP. The reaction was started by the addition of ATP. A unit of enzyme was defined as that amount which catalyzes the formation of 1 μmole of fructose 1,6-diphosphate (which in turn equals two μmoles of NADH oxidized) per minute under the conditions above. The specific activity was expressed as units of enzyme per mg of total intracellular protein.

4.5 Extracellular Enzyme Assays

The extracellular enzymes assayed were glucose dehydrogenase, gluconate dehydrogenase, and 2-KDG dehydrogenase, three membrane-bound enzymes discussed in Section 3.2. All three enzyme assays reactions involved the transfer of electrons from the substrate to an artificial electron acceptor, such as ferricyanide or NADP. In the cell, oxygen is the natural electron acceptor. The reduction of NADP to NADPH was observed by monitoring the change in absorbance at 340 nm with a spectrophotometer. The reduction of ferricyanide to ferrocyanide was observed by monitoring the change in absorbance at 660 nm.

4.5.1 Glucose Dehydrogenase

Glucose dehydrogenase catalyzes the oxidation of glucose to a glucono-δ-lactone, which in turn through a spontaneous hydrolysis reaction, turns into gluconate. The enzyme was assayed by following the formation of NADPH coupled with the oxidation

of glucose to glucono-δ-lactone (Mitamura, 1989). The overall reaction is shown in Equation 4-4 :

$$\text{glucose} + \text{NADP} \rightarrow \text{gluconate} + \text{NADPH} + H^{+} \qquad \textbf{4-4}$$

All reactions were carried out in 1 ml cuvettes at room temperature. The cuvette was placed in the spectrophotometer, and the reaction was started upon the addition of the active substrate. Upon the start of the reaction, absorbance readings at 340 nm were taken at 30-second intervals for 3 minutes. Control samples were performed to monitor the increase in absorbance due to background NADPH formation.

Concentrated glucose dehydrogenase was stable for at least 3 to 4 hours diluted in phosphate buffer (pH=6.5) containing 6 g/L potassium monobasic phosphate and 4 g/L potassium dibasic phosphate with 1% Triton X-100. The reaction mixture contained: 0.7 ml of phosphate buffer with 1% Triton X-100, 0.1ml of 1.5 mM NADP, 0.1 ml of glucose dehydrogenase (of known concentrations in U/ml), and 0.1 ml of various concentrations of glucose. The control mixture contained: 0.8 ml of phosphate buffer with 1% Triton X-100, 0.1 ml of 1.5 mM NADP, 0.1 ml of enzyme solution (of known concentrations in U/ml), and no glucose. The reaction was started by the addition of NADP. The absorbance measurements at 340 nm were converted to reaction velocity according to Equation 4-5, assuming a molar extinction coefficient of 6220 M^{-1} for NADPH and NADH (Mitamura, 1989).

$$\text{Velocity} = \frac{1000OD_{340}}{E_c t} \qquad \textbf{4-5}$$

Where Velocity = reaction velocity in mM/min

OD_{340} = absorbance change of reaction mixture in t minutes
E_c = molar extinction coefficient, 6220 M^{-1}
t = time allowed for reaction mixture to react, in min

4.5.2 Gluconate Dehydrogenase

Gluconate dehydrogenase catalyzes the oxidation of gluconate to 2-KDG. The enzyme is assayed by following the reduction of ferricyanide to ferrocyanide coupled with the oxidation of gluconate to 2-KDG (Wood, 1962). The overall reaction is shown in Equation 4-6:

$$\text{gluconate} + 2\ \text{ferricyanide} \rightarrow \text{2-KDG} + 2\ \text{ferrocyanide} \qquad \textbf{4-6}$$

Concentrated glucose dehydrogenase was stable diluted in 0.5 M sodium acetate (pH=5.5). The reaction mixture contained: 0.7 ml of 0.5 M sodium acetate (pH=5.5), 0.1 ml of 0.1 M ferricyanide, 0.1 ml of gluconate dehydrogenase (of known concentration), and 0.1 ml of various concentrations of gluconate. Control samples were performed to observe the change in absorbance due to background reduction of ferricyanide to ferrocyanide. The control mixture contained: 0.8 ml of 0.5 M sodium acetate (pH=5.5), 0.1 ml of 0.1 M ferricyanide, 0.1 ml of gluconate dehydrogenase (of known concentration), and no gluconate.

All reactions were carried out in 15-ml test tubes. One ml of reaction mixture was allowed to react for 10 minutes at room temperature after which time, 0.5 ml of ferric sulfate-Dupanol was added to stop the reaction. The mixture was allowed to stand at room temperature for 1 minute. Water was added to a total volume of 10 ml, and the absorbance reading at 660 nm was taken. The activity of gluconate dehydrogenase is

defined in units of enzyme per ml. One unit of enzyme is defined as the amount that causes the oxidation of 1 μmole of gluconate or the reduction of 2 μmoles of ferricyanide per minute. An absorbance reading of 1 equals 1 μmole of gluconate (Woods, 1962). The Ferric sulfate-Dupanol reagent contained 5 g of $Fe_2(SO_4)_3 \bullet n\text{-}H_2O$, 3 g of Dupanol (sodium lauryl sulfate), 95 ml of 85% phosphoric acid, and distilled water to 1000 ml.

4.5.3 2-KDG Dehydrogenase

2-KDG dehydrogenase catalyzes the oxidation of 2-KDG to form 2,5-DKG. The enzyme may be assayed by following the reduction of ferricyanide to ferrocyanide coupled with the oxidation of 2-KDG to 2,5-DKG (Shinagawa, 1981). The overall reaction is shown in Equation 4-7:

$$\text{2-KDG} + 2 \text{ ferricyanide} \rightarrow \text{2,5-DKG} + 2 \text{ ferrocyanide} \qquad \textbf{4-7}$$

Samples to be assayed for 2-KDG dehydrogenase contained either whole cells or membrane fractions. The whole cells or membrane fractions were harvested and washed with and finally resuspended in 0.5 M sodium acetate (pH=5.5). The reaction mixture contained: 0.7 ml of 0.5 M sodium acetate (pH=5.5), 0.1 ml of 0.1 M ferricyanide, 0.1 ml of crude enzyme sample, and 0.1 ml of various concentrations of 2-KDG. Control samples were performed to observe the change in absorbance due to background reduction of ferricyanide to ferrocyanide. The control mixture contained: 0.8 ml of 0.5 M sodium acetate (pH=5.5), 0.1 ml of 0.1 M ferricyanide, 0.1 ml of crude enzyme sample, and no 2-KDG.

All reactions were carried out in 15-ml test tubes. One ml of reaction mixture was allowed to react for 10 minutes at room temperature, after which time 0.5 ml of ferric sulfate-Dupanol was added to stop the reaction. The mixture was allowed to stand at room temperature for 1 minute. Water was added to bring the total volume to 10 ml, and the absorbance reading at 660 nm was taken. The activity of 2-KDG dehydrogenase is defined in units of enzyme per ml. One unit of enzyme is defined as the amount that causes the oxidation of 1 μmole of 2-KDG or the reduction of 2 μmoles of ferricyanide per minute. An absorbance reading of 1 equals 1 μmole of 2-KDG (Woods, 1962).

4.6 Protein Determination

Intracellular, membrane, and total cellular protein content were determined. Protein was determined by following the colorimetric method enclosed in a commercially available protein assay kit (BioRad, Hercules, CA). Lyophilized bovine serum albumin was used as a standard.

4.7 Batch Experiments

Batch experiments to produce 2,5-DKG from glucose using *P. citrea* were performed in a New Brunswick Bioflow 3000 bioreactor (Edison, NJ). Bioreactor rotational agitation speed was held constant at 1000 RPM. Temperature was held constant at 28 °C. The pH was controlled at 5.8 using 2 M KOH. Air was fed at 2.5 L/min. Dissolved oxygen was not controlled but monitored. The medium used in all batch experiments consisted of 20 g/L potassium monobasic phosphate buffer with 25 g/L glucose. 2,5-DKG concentration in the reactor was measured once an hour by taking

a 20-ml sample. The experiment was stopped once the 2,5-DKG concentration no longer increased over time.

4.7.1 Cell Growth for Batch Experiments

Cells used in these batch experiments were generated in the bioreactor under the above conditions (Section 4.7). The 4-L final growth media was made of two portions. The 3.6-L autoclavable portion consisted of: 18.4 g KH_2PO_4, 3.2 g $MgSO_4 \bullet 7H_2O$, 18.8 g $(NH_4)_2SO_4$, 30 g glutamic acid, and 0.224 g choline chloride in 3.2 L of water. The 0.4-L remaining portion consisted of 48.43 g fructose, 66.87 g glucose, and 33.4 mg nicotinic acid in 200 ml of water sterilized using a filter with 0.2 micron pore size. Cells were harvested when they reached stationary phase, usually after 10-12 hours, indicated by an increase in dissolved oxygen, as shown in Figure 4-1. Cells were centrifuged at 10,000 RPM for 25 minutes and resuspended with 10 g/L monophosphate buffer. The cell pellet was harvested by centrifugation at 10,000 RPM for 25 minutes, and the supernatant was discarded. The pellet was collected and stored at -80 °C.

4.7.2 Preparations of Nonviable Cells

Batch experiments for the production of 2,5-diketogluconate were also performed using membrane fractions and permeabilized cells. To prepare the membrane fractions, cells were first resuspended in 10 g/L monophosphate buffer. The absorbance at 600 nm of a 1-ml thousand-fold dilution of cell suspension was 0.1. The optical density of the undiluted cell mixture would therefore have been 100. The cell mixture was passed through a French press (SLM Instruments, Urbana, IL) twice and subsequently

ultracentrifuged at 25,000 RPM for 2 hours (Gerhardt, 1994). The precipitated membrane fraction was saved and stored at -80 °C.

Permeabilized cells are another form of nonviable cells. The cell membrane is rendered permeable to various compounds by chemical treatment. To prepare the permeabilized cells, the cells were resuspended with monophosphate buffer. The absorbance at 600 nm of a 1-ml thousand fold dilution of cell suspension was 0.1. The optical density of the cell mixture was calculated to be 100. To every 1 ml of OD100 cell suspension, 0.1 ml of the permeabilizing agent consisting of 90% acetone, and 10% toluene, was added. The cell suspension was shaken vigorously and centrifuged at 11,000 RPM for 25 minutes (Gerhardt, 1994). After discarding the supernatant, the pellet was resuspended with monophosphate buffer. The mixture was centrifuged again at 11,000 RPM for 25 minutes. The supernatant was again discarded and the permeabilized cell pellets stored at -80 °C.

4.8 Analytical Methods

2,5-DKG content in batch experiment samples was determined by high pressure liquid chromatography (HPLC). Samples were analyzed with a Perkin-Elmer (Norwalk, CT) LC-235 Diode Array Detector at 210 nm. The column used for separation was a SupelcoGel H ion exchange column (Supelco, Bellefonte, CA). A solution of 0.5% phosphoric acid flowing at 0.35 mL/min served as eluent for the isocratic separation with a run time of 20 minutes.

Glucose content in batch experiment samples were determined using a Dionex HPLC system consisting of an LC 20 chromatography enclosure, an ED 40

electrochemical detector running in amperometry mode, an AD 40 autosampler, and a GP 40 gradient pump. A CarboPac PA10 ion exchange column was used for the separation. A solution of 100 mM NaOH flowing at 1 mL/min served as eluent for the isocratic separation with a run time of 15 minutes (Dalton, 1999).

5 Mathematical Model Studies

5.1 Mathematical Model for the Batch Production of 2,5-DKG

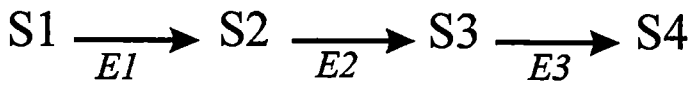
A mathematical model for the batch production of 2,5-DKG was derived based on the kinetics of the enzymes responsible for 2,5-DKG. The kinetic mechanism proposed was based on simple Michaelis-Menten kinetics (Figure 5-1). The concentration over time of each species involved in 2,5-DKG production was described using the Michaelis-Menten equation (Equation 3-6). A mass balance equation in the form of an ordinary differential equation (ODE) can be written to account for the concentration of each species formed or consumed over time.

In batch production experiments performed, glucose was the only species present at time zero. Glucose, then, was converted into 2,5-DKG through the three dehydrogenase enzymes. Given the initial concentrations of each species, initial and final time, the mass balance equations may be solved simultaneously to yield the concentration profiles of each species over time. The equations were solved numerically using the ODE solver software Polymath (Madison, WI) by a built-in third-order Runga-Kutta method.

5.1.1 Mass Balance on Glucose

In the case of batch experiments using whole cells, the concentration of glucose in the reactor at any time may be described by two degradation terms. The concentration of

Enzymatic Reaction Schematic &
Kinetic Mechanism Proposed



1) S1 + E1 ↔ S1E1 — *S1 forms a complex with E1*
2) S1E1 ↔ S2 + E1 — *S1E1 complex yields S2*
3) S2 + E2 ↔ S2E2 — *S2 forms a complex with E2*
4) S2E2 ↔ S3 + E2 — *S2E2 complex yields S3*
5) S3 + E3 ↔ S3E3 — *S3 forms a complex with E3*
6) S3E3 ↔ S4 + E3 — *S3E3 complex yields S4*

S1 = Glucose — *E1 = Glucose dehydrogenase*
S2 = Gluconate — *E2 = Gluconate dehydrogenase*
S3 = 2-KDG — *E3 = 2-KDG dehydrogenase*
S4 = 2,5-DKG

Figure 5-1 The enzymatic model schematic and the kinetics proposed

glucose in the reactor at any time may be described by the following:

$$\frac{d[S_1]}{dt} = -\frac{k_{\max}^{E_1}[E_1][S_1]}{K_M^{E_1} + [S_1]} - \frac{U_T[X][S_1]}{K_M^{U_T} + [S_1]} \qquad \textbf{5-1}$$

Where

$[S_1]$ = concentration of glucose in mM

$[E_1]$ = total enzyme concentration of glucose dehydrogenase in U/mL

$k_{\max}^{E_1}$ = maximum specific rate constant of glucose dehydrogenase in μmole/min/U

K_M^{E1} = Michaelis constant of glucose dehydrogenase in mM

U_T = maximum specific rate constant for the uptake of glucose in millimole of glucose/min/g of dry weight of cells

[X] = concentration of cells in g dry weight /L

$K_M^{U_T}$ = half saturation constant for glucose uptake in mM

The first term in Equation 5-1 is the degradation of glucose by the enzyme glucose dehydrogenase and is described by Michaelis-Menten kinetics. The second term describes the glucose uptake into viable cells. The portion of glucose utilization by pathways associated with central metabolism is modeled as a Michaelis-Menten type saturational kinetics, with U_T as the maximum specific rate constant for the glucose uptake, and $K_M^{U_T}$ as the half saturation constant.

The glucose uptake rate constant U_T for the *P. citrea* strain has not yet been reported in literature. The value of the uptake of glucose in *E. coli* has been reported to be 0.0014 min^{-1} (Chou, 1994) In this study, gluconate, 2-KDG, or even 2,5-DKG uptakes into the cell may also exist. However, these uptakes were not incorporated into the model. U_T is a rate constant that represents the uptake of all species not involved in the production of 2,5-DKG into the cell in the form of glucose. Glucose uptake is modeled as a pseudo-first order reaction with respect to the cell mass and zero order with respect

to glucose concentration. In order to model glucose uptake in an equation whose independent variable is glucose concentration using Polymath, the equation solver package used to solve the model equations, an approximation must be made.

In this work, the $K_M^{U_i}$ is assumed to be infinitely smaller than the substrate concentration in Equation 5.1 to facilitate the solving of the model equations in Polymath.. Thus the two glucose concentrations in the second terms of Equation 5.1 cancel each other, and a pseudo-first order with respect to the cell mass and zero order with respect to glucose concentration is effectively established. By doing so, any negative concentration values that may otherwise arise as the model is solved may effectively be eliminated. As a result, the uptake of glucose is modeled as a pseudo-first order reaction with respect to cell concentration with a uptake rate constant, U_T. And

In the case of nonviable cells, central metabolism is no longer an issue to be considered. U_T is zero in this case, and the concentration of glucose may be described by simply the first degradation term only.

5.1.2 Mass Balance on Gluconate

The concentration of gluconate at any time may be described by two terms. It is not only produced by the first reaction catalyzed by glucose dehydrogenase, but also degraded by the second reaction catalyzed by gluconate dehydrogenase. The rate of 2-KDG formation was assumed to equal the rate of gluconic acid degradation.

$$\frac{d[S_2]}{dt} = \frac{k_{\max}^{E_1}[E_1][S_1]}{K_M^{E_1} + [S_1]} - \frac{k_{\max}^{E_2}[E_2][S_2]}{K_M^{E_2} + [S_2]} \qquad \text{5-2}$$

Where

$[S_2]$ = concentration of gluconate in mM

$[E_2]$ = total enzyme concentration of gluconate dehydrogenase in U/mL

$k_{\max}^{E_2}$ = maximum specific rate constant of gluconate dehydrogenase in μmole/min/U

$K_M^{E_2}$ = Michaelis constant of gluconate dehydrogenase in mM

5.1.3 Mass Balance on 2-KDG

The concentration of 2-KDG in the reactor at any time may be described by two terms. It is not only produced by the second reaction catalyzed by gluconate dehydrogenase, but also degraded by the third reaction catalyzed by 2-KDG dehydrogenase. The rate of 2,5-DKG formation is assumed to equal the rate of 2-KDG degradation.

$$\frac{d[S_3]}{dt} = \frac{k_{\max}^{E_2}[E_2][S_2]}{K_M^{E_2} + [S_2]} - \frac{k_{\max}^{E_3}[E_3][S_3]}{K_M^{E_3} + [S_3]} \qquad \text{5-3}$$

Where

$[S_3]$ = concentration of 2-KDG in mM

$[E_3]$ = total enzyme concentration of 2-KDG dehydrogenase in U/mL

$k_{\max}^{E_3}$ = rate constant associated 2-KDG dehydrogenase in μmole/min/U

$K_M^{E_3}$ = Michaelis constant of 2-KDG dehydrogenase in mM

5.1.4 Mass Balance on 2,5-DKG

The concentration of 2,5-DKG in the reactor at any time may be described by one term. It is only produced by the third reaction catalyzed by 2-ketogluconate dehydrogenase and is not degraded.

$$\frac{d[S_4]}{dt} = \frac{k_{\max}^{E_3}[E_3][S_3]}{K_M^{E_3} + [S_3]} \qquad \text{5-4}$$

where $[S_4]$ = concentration of 2,5-DKG in mM

5.2 Determination of Kinetic Parameters

Kinetic parameters for glucose dehydrogenase, gluconate dehydrogenase, and 2-KDG dehydrogenase were determined experimentally. For each enzyme, initial rate experiments described in Section 4.5 were performed at two known enzyme concentrations. The K_m and V_{max} for each enzymes were determined from the Lineweaver-Burke plots (Stryer, 1995). k_{max} was determined by normalizing V_{max} to the amount of enzymes used. In the following, K_m and k_{max} for each enzyme will be shown to be independent from the enzyme concentration.

5.2.1 Kinetic Parameters for Glucose Dehydrogenase

Initial rate experiments were performed at two different enzyme concentrations, 2.5 U/ml and 1.25 U/ml. The concentrations of the substrate glucose used were: 100 mM, 50 mM, 25 mM, 10 mM, 5 mM, 1 mM, and 0.5 mM. The change in absorbance at 340 nm, due to the formation of NADPH, was monitored over two minutes. This was corrected by subtracting the change in absorbance in the control samples, the result of the background formation of NADPH. The corrected change in absorbance was converted to moles of NADPH formed by using the molar extinction coefficient, 6220 M^{-1}. From the Lineweaver-Burk plot in Figure 5-2, values for K_m and k_{max} for glucose dehydrogenase were determined to be 13.26 mM and 0.0749 μmol/min/U, respectively. The Michaelis-Menten equation, using these two parameters derived from experimental data, was

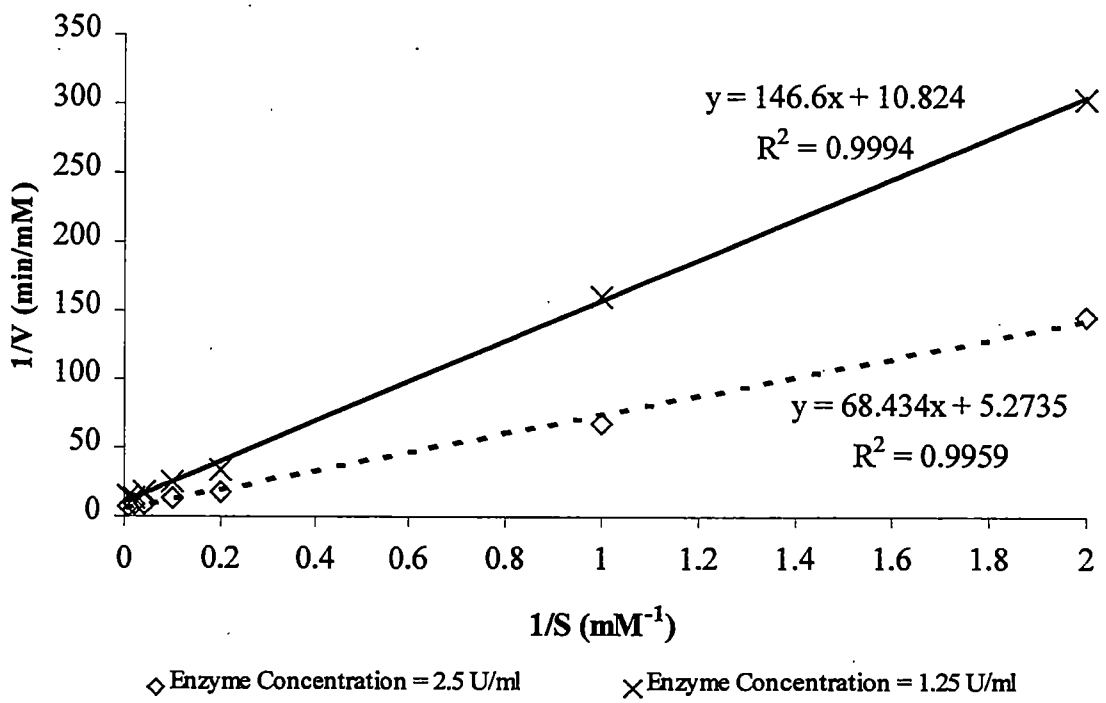


Figure 5-2 Lineweaver-Burk plot for initial-rate experiments conducted with two enzyme concentrations of glucose dehydrogenase, obtained from *Bacillus megaterium*

written for glucose dehydrogenase in order to predict the velocity at each substrate concentration:

$$V = \frac{0.0749[E][S]}{13.26 + [S]} \qquad \text{5-5}$$

Where [E] = the glucose dehydrogenase concentration in U/ml
[S] = substrate concentration in mM
V = velocity in mM/min
0.0749 in μmol/min/U
13.26 in mM

Figure 5-3 and Figure 5-4 show both experimentally-determined velocities and the velocities predicted by Equation 5-5 which utilizes Michaelis-Menten parameters derived from Lineweaver-Burk plots at two different enzyme concentrations. Equation 5-5 predicted the values of experimental velocities at two enzyme concentrations very well, indicating that Michaelis-Menten equation adequately describes the initial rates of glucose dehydrogenase kinetics.

5.2.2 Kinetic Parameters for Gluconate Dehydrogenase

Initial rate experiments were performed at two different enzyme concentrations, 1.25 U/ml and 0.625 U/ml. The concentrations of the substrate gluconate used were: 100 mM, 50 mM, 25 mM, 10 mM, 5 mM, 1 mM, and 0.5 mM. The change in absorbance at 660 nm was due to the reduction of ferricyanide to ferrocyanide. This was corrected by subtracting the change in absorbance in the control samples, the result of the background formation of ferrocyanide. The concentration of gluconate oxidized or 2-KDG formed

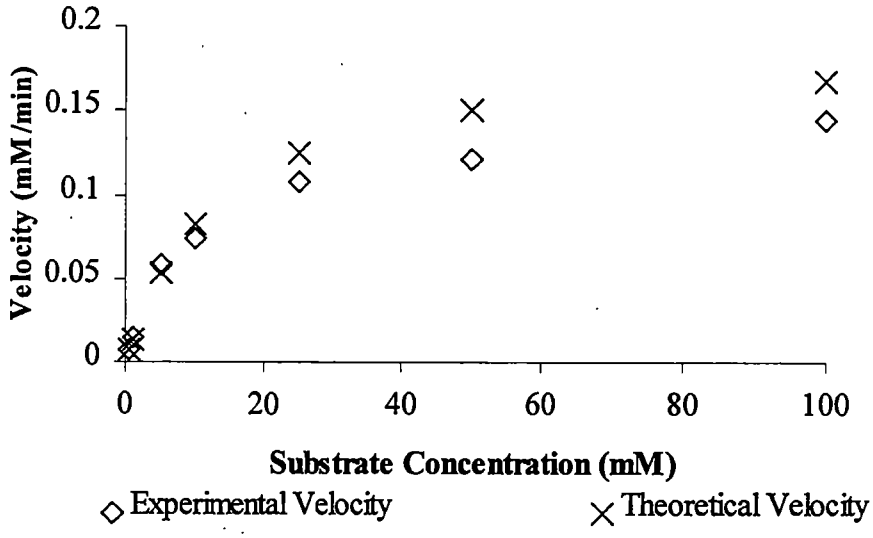


Figure 5-3 Comparison of experimentally measured velocities and predicted velocities using parameters derived from Lineweaver-Burk plot at glucose dehydrogenase concentration of 2.5 U/mL

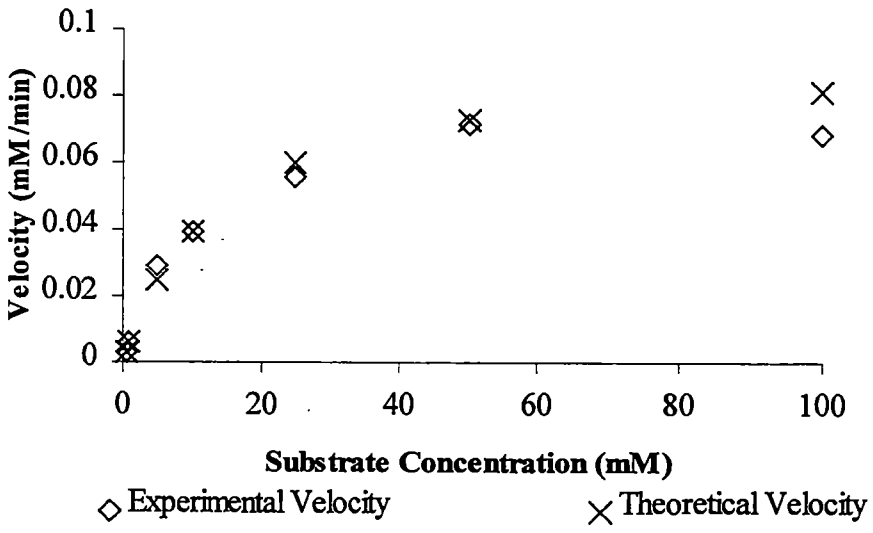


Figure 5-4 Comparison of experimentally measured velocities and predicted velocities using parameters derived from Lineweaver-Burk plot at glucose dehydrogenase concentration of 1.25 U/ml

was obtained from the absorbance reading (Section 4.5.2). From the Lineweaver-Burk plot in Figure 5-5, values for K_m and k_{max} were determined to be 4.127 mM and 0.0147 μmol/min/U, respectively. The Michaelis-Menten equation was written for gluconate dehydrogenase using these two parameters derived from experimental data. Equation 5-6 was used to predict the velocity at each substrate concentration:

$$V = \frac{0.0147[E][S]}{4.127 + [S]} \qquad \textbf{5-6}$$

Where E = the gluconate dehydrogenase concentration in U/ml
S = substrate concentration in mM
V = velocity in mM/min
0.0147 in μmol/min/U
4.127 in mM

Figure 5-6 and Figure 5-7 showed both experimentally-determined velocities and the velocities predicted by Equation 5-6. Equation 5-6 predicted the values of experimental velocities at two enzyme concentrations very well, indicating that Michaelis-Menten equation adequately describes the initial rates of gluconate dehydrogenase kinetics.

5.2.3 Kinetic Parameters for 2-KDG Dehydrogenase

Initial rate experiments were performed at two different enzyme concentrations, 18.9 U/ml and 11.9 U/ml. The concentration of the substrate gluconate used were: 100 mM, 50 mM, 25 mM, 10 mM, 5 mM, 1 mM, and 0.5 mM. The change in absorbance at 660 nm was due to the reduction of ferricyanide to ferrocyanide. This was corrected by subtracting the change in absorbance in the control samples, the result of he background formation of ferrocyanide. The concentration of 2-KDG oxidized or 2,5-DKG formed was obtained from the absorbance reading (Section 4.5.3). From the Lineweaver Burke

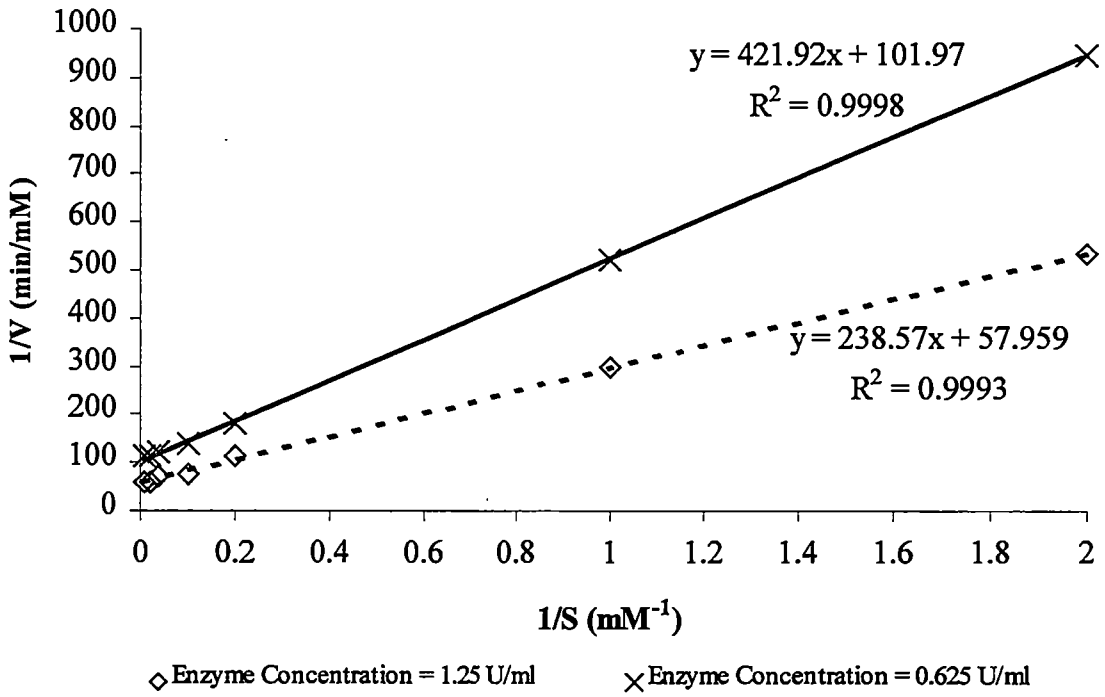


Figure 5-5 Lineweaver-Burk plot for initial-rate experiments conducted with two enzyme concentrations of gluconate dehydrogenase, obtained from *Pseudomonas sp.*

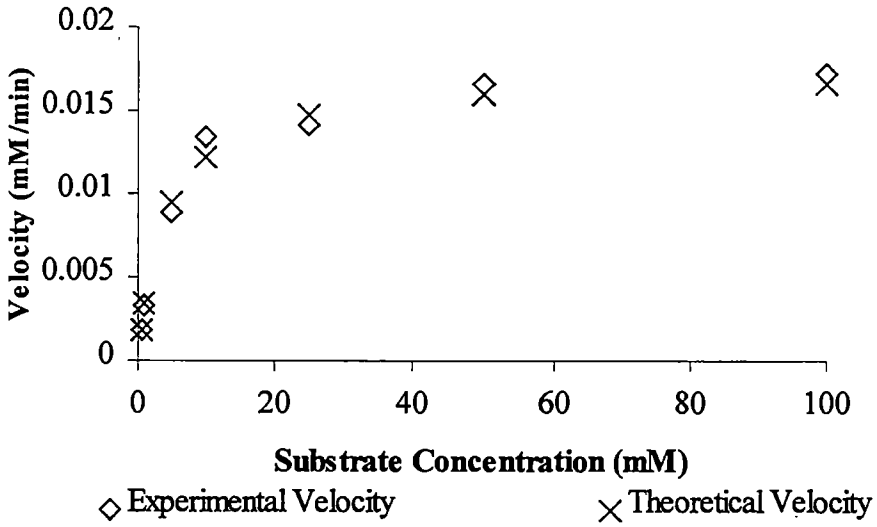


Figure 5-6 Comparison of experimentally measured velocities and predicted velocities using parameters derived from Lineweaver-Burk plot at gluconate dehydrogenase concentration of 1.25 U/m

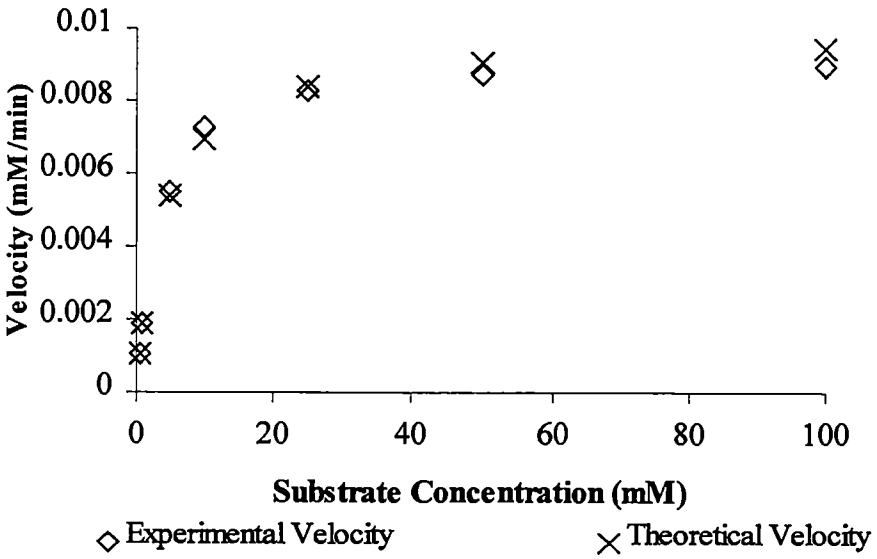


Figure 5-7 Comparison of experimentally measured velocities and predicted velocities using parameters derived from Lineweaver-Burk plot at gluconate dehydrogenase concentration of 0.625 U/m

plot in Figure 5-8, values for K_m and k_{max} were determined to be 2.307 mM and 0.0139 μmol/min/U, respectively. The Michaelis-Menten equation, using these two parameters derived from experimental data, was written again for 2-KDG dehydrogenase in order to predict the velocity at each substrate concentration:

$$V = \frac{0.0139[E][S]}{2.307 + [S]} \qquad \textbf{5-7}$$

Where [E] = the 2-KDG dehydrogenase concentration in U/ml
[S] = substrate concentration in mM
V = velocity in mM/min
0.0139 in μmol/min/U
2.307 in mM

As Figure 5-9 and Figure 5-10 both show, values of experimentally determined velocities and those velocities predicted by Equation 5-7 were very similar. Equation 5-7 predicted the values of experimental velocities at two enzyme concentrations very well, indicating that Michaelis-Menten equation adequately describes the initial rate for 2-KDG dehydrogenase kinetics.

Table 5-1 is a summary of all of the experimentally determined kinetic parameters for the enzymes in the 2,5-DKG production pathway.

Table 5-1 Experimentally Determined Kinetic Parameters for the Enzymes in 2,5-DKG Production Pathway

	K_m (mM)	k_{max} (μmol/min/U)
Glucose dehydrogenase	13.26	0.0749
Gluconate dehydrogenase	4.127	0.0147
2-ketogluconate dehydrogenase	2.307	0.0139

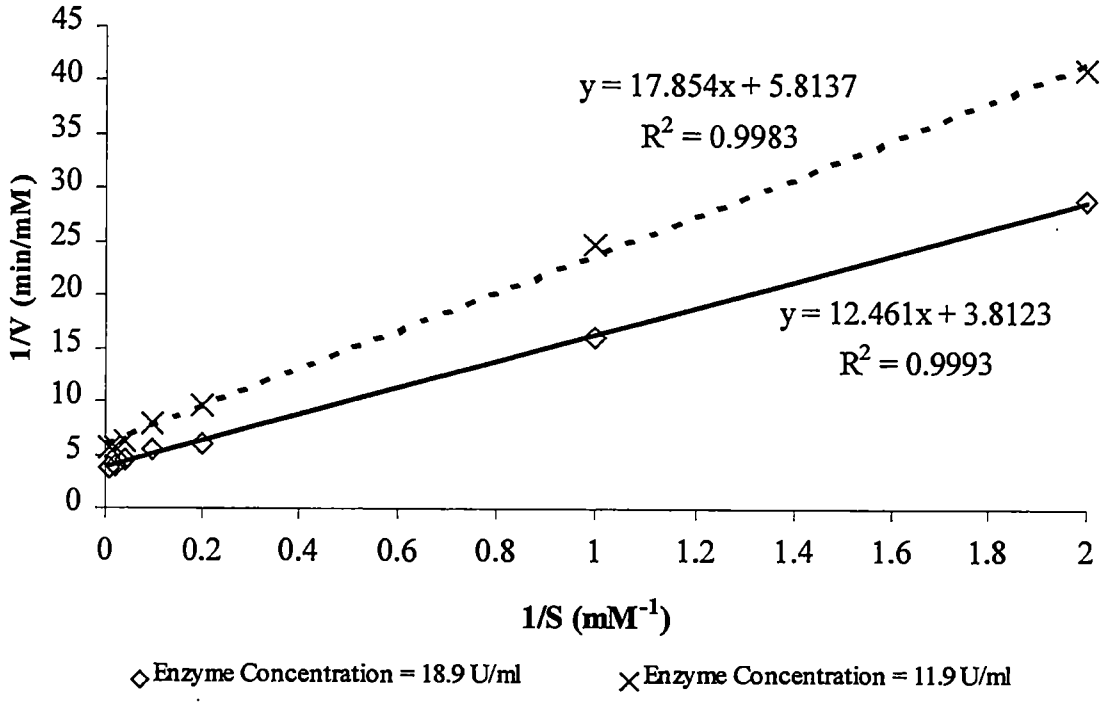


Figure 5-8 Lineweaver-Burk plot for initial-rate experiments conducted with two enzyme concentrations of 2-KDG dehydrogenase, from *Pantoea citrea*

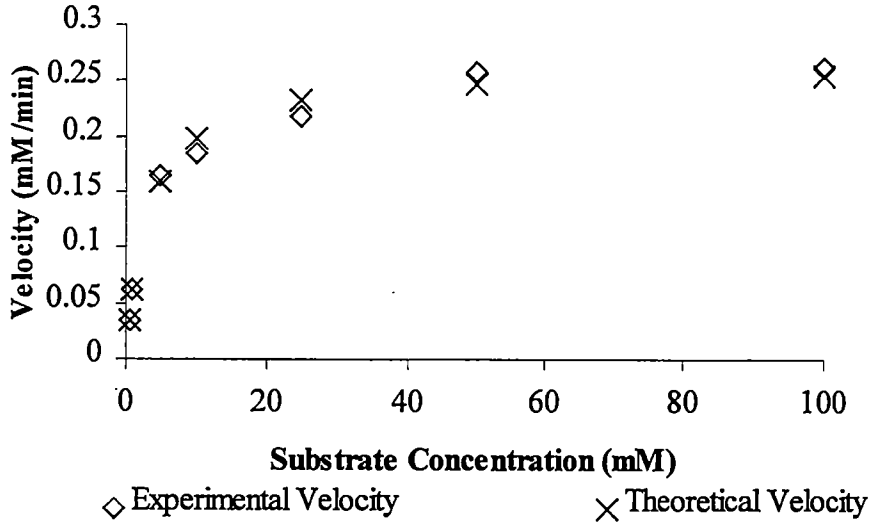


Figure 5-9 Comparison of experimentally measured velocities and predicted velocities using parameters derived from Lineweaver-Burk plot at 2-KDG dehydrogenase concentration of 18.9 U/m

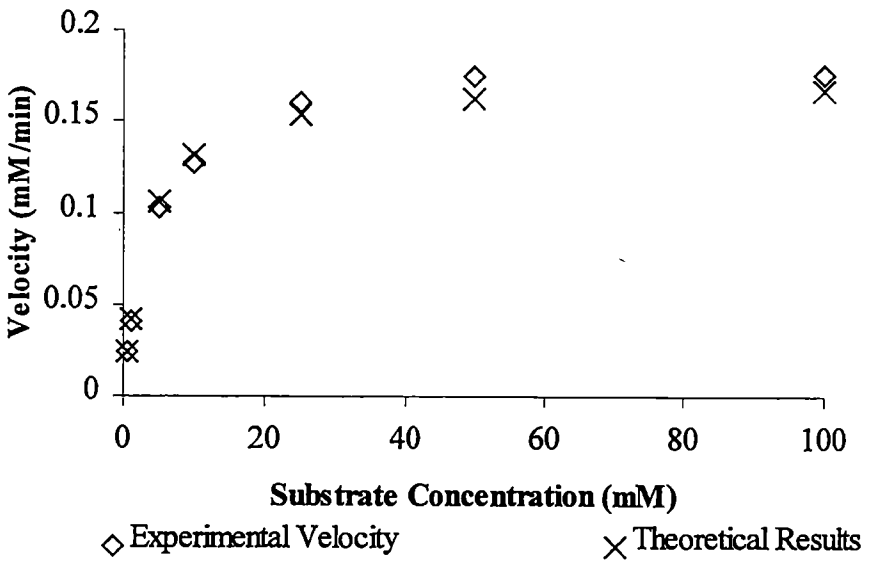


Figure 5-10 Comparison of experimentally measured velocities and predicted velocities using parameters derived from Lineweaver-Burk plot at 2-KDG dehydrogenase concentration of 11.9 U/m

6 Results

6.1 Growth Characteristics of *P. citrea*

Growth rates of *P. citrea* on various substrates were determined. Substrates used in the experiment were glucose, fructose, gluconate, equal amounts of glucose and fructose, and equal amounts of glucose and gluconate. Using a spectrophotometer, absorbance readings taken once an hour at 600 nm and were correlated to dry weight concentrations as shown in Figure 6-1. According to the growth curve in Figure 6-2, the highest final cell mass concentration achieved was 0.8 ± 0.3 mg dw/ml. The substrate was either fructose, gluconate, or the combination of fructose and glucose. When the substrate was a combination of glucose and gluconate, the final cell mass concentration was 0.69 mg dw/ml. When the substrate was glucose, the final cell mass concentration was 0.42 mg dw/ml, about half of that when the substrate was fructose. Compared to fructose, glucose was not a very good substrate for the growth. Table 6-1 lists the maximum cell growth rates and substrate yield. The substrate yield for glucose (0.089) was half of the substrate yield for all other substrates (0.17). The maximum growth rate (4.25 hr^{-1}) was exhibited when the substrate was fructose. The minimum growth rate (0.15 hr^{-1}) was exhibited when the substrate was glucose.

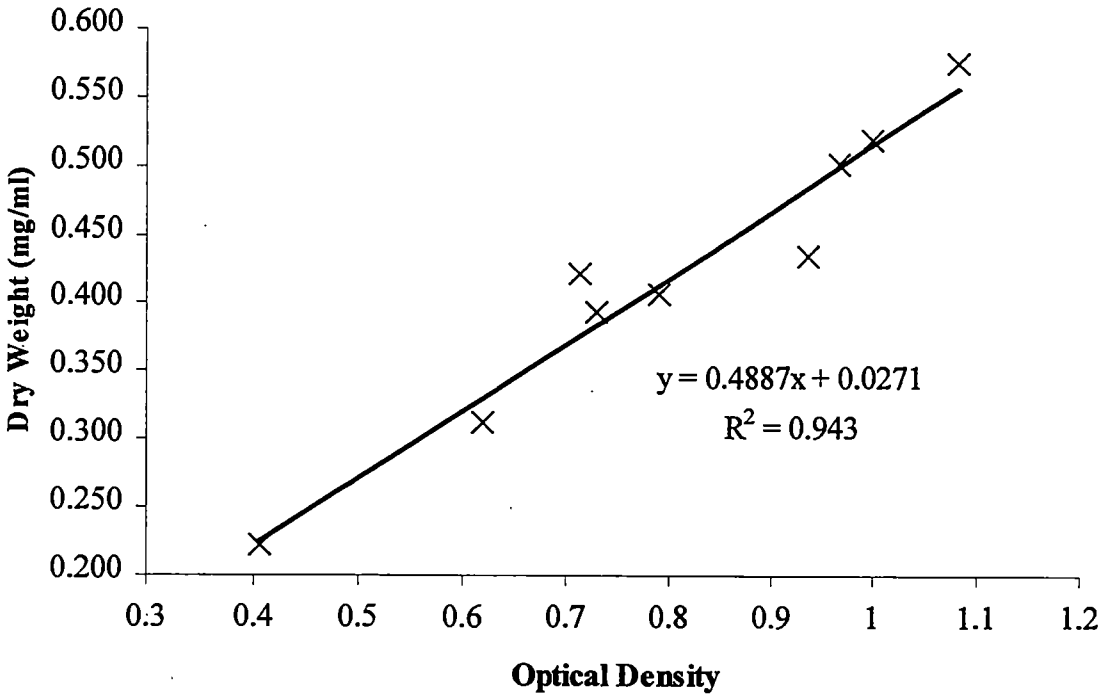


Figure 6-1 Optical density and cell concentration (mg dw/ml) for *P. citrea*

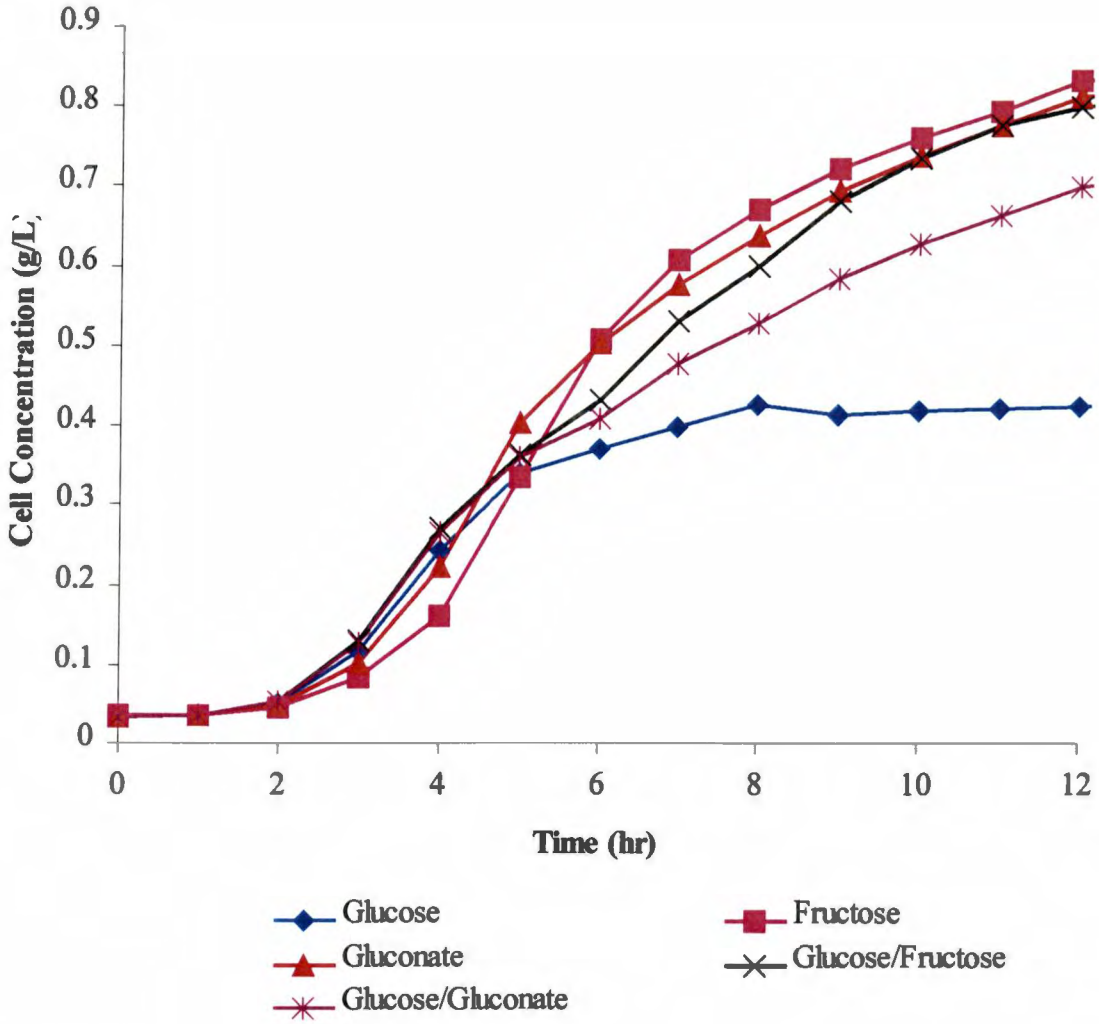


Figure 6-2 Growth curve of *P. citrea* on various carbohydrate substrates

Table 6-1 Growth Characteristics of *P. citrea* on Various Carbohydrates

	Max Growth Rate (hr^{-1})	Substrate Yield (g dw/g)
Glucose	0.15	0.089
Fructose	4.25	0.17
Gluconate	1.01	0.17
Glucose/Fructose	0.89	0.17
Glucose/Gluconate	1.10	0.16

6.2 Enzyme Activities of *P. citrea* and *E. coli* in Log Phase

The purpose of this set of experiments was to determine the relative activities of the major pathways of glucose catabolism in *P. citrea* during log phase growth. Comparisons of these activities were made to those in *E. coli* which was used as a positive control and a verification of the assay methods because all of the major pathways considered exist in *E. coli.*

The cell-free extract used for the enzyme assays was prepared as outlined in Section 4.3. The activities of the enzymes assayed were all normalized to total intracellular protein in milligrams. Table 6-2 lists the activity of each key enzyme(s) of *P. citrea* cells, grown on different substrates, in log growth phase. The external 2,5-DKG pathway exhibited high activity, and appeared to be independent of the substrate on which the cells were grown. Of the internal pathways, the PP pathway appeared to be the most active pathway of the three no matter what substrate *P. citrea* was grown on (see Figure 3-1 for details of pathways). The PP pathway was the most active when the substrate was pyruvate. The EMP pathway was the most active when the substrate was

glucose. The ED pathway did not reflect the highest activity when the substrate was gluconate. This was not observed in *E. coli*.

Table 6-2 Relative Activities of Internal Metabolic Pathways in *P. citrea* in Growth Phase Grown on Various Carbohydrates

	PP Pathway (U/mg)	ED Pathway (U/mg)	EMP Pathway (U/mg)	DKG Pathway (U/mg)
Glucose	0.42 ± 0.0039	0.11 ± 0.013	0.23 ± 0.070	16.6 ± 4.2
Fructose	0.32 ± 0.038	0.19 ± 0.032	0.15 ± 0.043	16.6 ± 4.2
Gluconate	0.39 ± 0.080	0.08 ± 0.049	0.16 ± 0.049	-
Pyruvate	0.50 ± 0.068	0.15 ± 0.023	0.19 ± 0.030	-

Table 6-3 listed the activity of each key enzyme(s) of *E. coli* cells, grown on different substrates, in growth phase. The PP pathway was no longer the most active pathway of the three. The PP pathway was the most active when the substrate was glucose and pyruvate. The EMP pathway was the most active when the substrate was glucose and gluconate. The EMP pathway was the most active pathway of the three no matter what substrate E. coli was grown on. The ED pathway was the most active when the substrate was gluconate.

Table 6-3 Relative Activities of Internal Metabolic Pathways in *E. coli* in Growth Phase Grown on Various Carbohydrates

	PP Pathway (U/mg)	ED Pathway (U/mg)	EMP Pathway (U/mg)	DKG Pathway (U/mg)
Glucose	0.37 ± 0.016	0.24 ± 0.11	0.47 ± 0.040	0
Fructose	0.17 ± 0.020	0.019 ± 0.080	0.25 ± 0.020	0
Gluconate	0.30 ± 0.0060	0.37 ± 0.035	0.40 ± 0.060	0
Pyruvate	0.32 ± 0.0050	0.16 ± 0.38	0.54 ± 0.027	0

6.3 Enzyme Activities of *P. citrea* in Stationary Phase

The purpose of this set of experiments was to determine the relative activities of the major pathways of glucose catabolism in *P. citrea* during stationary phase. The cell-free extract for enzyme assays was prepared as outlined in Section 4.3. Membrane and intracellular protein in mg/ml were also measured. The specific activities of the enzymes assayed were all normalized to total intracellular protein in milligrams.

All parameters measured stayed relatively constant over the 5 hours (Table 6-4). The standard deviations all fell within ±20% of the mean. As in log phase, the PP pathway was still very active in stationary phase. The enzyme activities for the PP and EMP pathways in stationary phase were nearly identical to those in log phase. The 2,5-DKG pathway was still the most active of the pathways considered.

Table 6-4 Relative Activities of Internal Metabolic Pathways in *P. citrea* in Stationary Phase with Various Air Flow Rates

	Glucose
EMP Pathway(U/mg)	0.25 ± 0.062
PP Pathway (U/mg)	0.42 ± 0.13
DKG Pathway (U/mg)	14.82 ± 3.7
Membrane Protein (mg/mL)	1.74 ± 0.42
Intracellular Proteins (mg/mL)	1.82 ± 0.35

The enzyme activity measurements showed that the PP pathway has a higher activity than the EMP and ED pathways in *P. citrea* in both log growth and stationary phases. However, the highest activity was exhibited in the extracellular 2,5-DKG production pathway. The low activity of the internal glucose metabolism pathways, coupled with poor growth rate on glucose, and high activity of the 2,5-DKG pathway,

suggested that the glucose is channeled through the extracellular pathway and thus prevented from entering central metabolism in *P. citrea.*

6.4 Batch Production of 2,5-DKG

The enzyme assays indicated that the majority of the glucose was channeled through the 2,5-DKG pathway during both log growth and stationary phases. A portion of the total glucose fed was channeled through central metabolism. The purpose of this set of batch experiments was to investigate the effect of central metabolism on the batch conversion of glucose to 2,5-DKG.

The overall conversion of glucose to 2,5-DKG was obtained from batch productions of 2,5-DKG using both viable and nonviable *P. citrea* cells. Nonviable forms of *P. citrea* used were permeabilized cells and cellular membrane fractions. All experiments were performed with an initial glucose concentration of 25 g/L. The actual working volume of the reactor was 2 L. Approximately 20 mL of reactor broth was taken once an hour to be analyzed for glucose and 2,5-DKG content. The experiment was terminated once the 2,5-DKG concentration stopped increasing over time. The final volume of the reactor broth was measured. The total formation of 2,5-DKG in mass was calculated by taking into consideration the 2,5-DKG in both the final reactor broth as well as each sample taken. Theoretically, 100% conversion of 50 g (25 g/L of initial glucose concentration in 2 L of working reactor volume) of glucose would yield a total of 53.33 g of 2,5-DKG. Percentage of overall conversion for each fermentation was determined by dividing the total measured experimental formation of 2,5-DKG by the theoretical total formation.

6.4.1 Batch production of 2,5-DKG using whole cells of *P. citrea*

By using whole cells of *P. citrea* in the batch production of 2,5-DKG, the effect of central metabolism on the overall conversion of glucose to 2,5-DKG was determined. The overall conversion of glucose to 2,5-DKG using whole cells was calculated to be 75.46 ± 1.92 %. A total of four experiments were performed, two at lower cell concentrations (the absorbance taken at 600 nm of a 1 to 10 dilution was 0.5) and two at higher cell concentrations (the absorbance at 600 nm of a 1 to 10 dilution was 0.8). The cell concentration in the reactor was quantified by the enzyme concentration (U/ml) of 2-KDG dehydrogenase present. The volumetric 2-KDG dehydrogenase activity in the reactor was measured (Section 4.5.3) at both the beginning and end of each experiment, and was found to be fairly constant throughout. The volumetric enzyme activity and total protein measurements are listed in Table 6-5. All measurements remained fairly constant throughout the experiment.

Table 6-5 Volumetric 2-KDG Dehydrogenase Enzyme Activity and Protein Concentration at the Beginning and End of Batch Production of 2,5-DKG Using Whole Cells

	Cell Conc.	Beginning	End
Volumetric Activity (U/ml)	Low (OD=5)	15.95 ± 0.45	16.79 ± 0.91
Protein Concentration (mg/ml)		0.38 ± 0.055	0.38 ± 0.044
Specific activity (U/mg)		42.13 ± 1.12	43.94 ± 2.39
Volumetric Activity (U/ml)	High (OD=8)	24.6 ± 0.36	25.27 ± 0.83
Protein Concentration (mg/ml)		0.65 ± 0.08	0.59 ± 0.06
Specific activity (U/mg)		37.77 ± 0.28	40.48 ± 0.57

Figure 6-3 shows the reactor concentrations of glucose and 2,5-DKG over time in the two experiments conducted at the lower cell concentration. The two batch

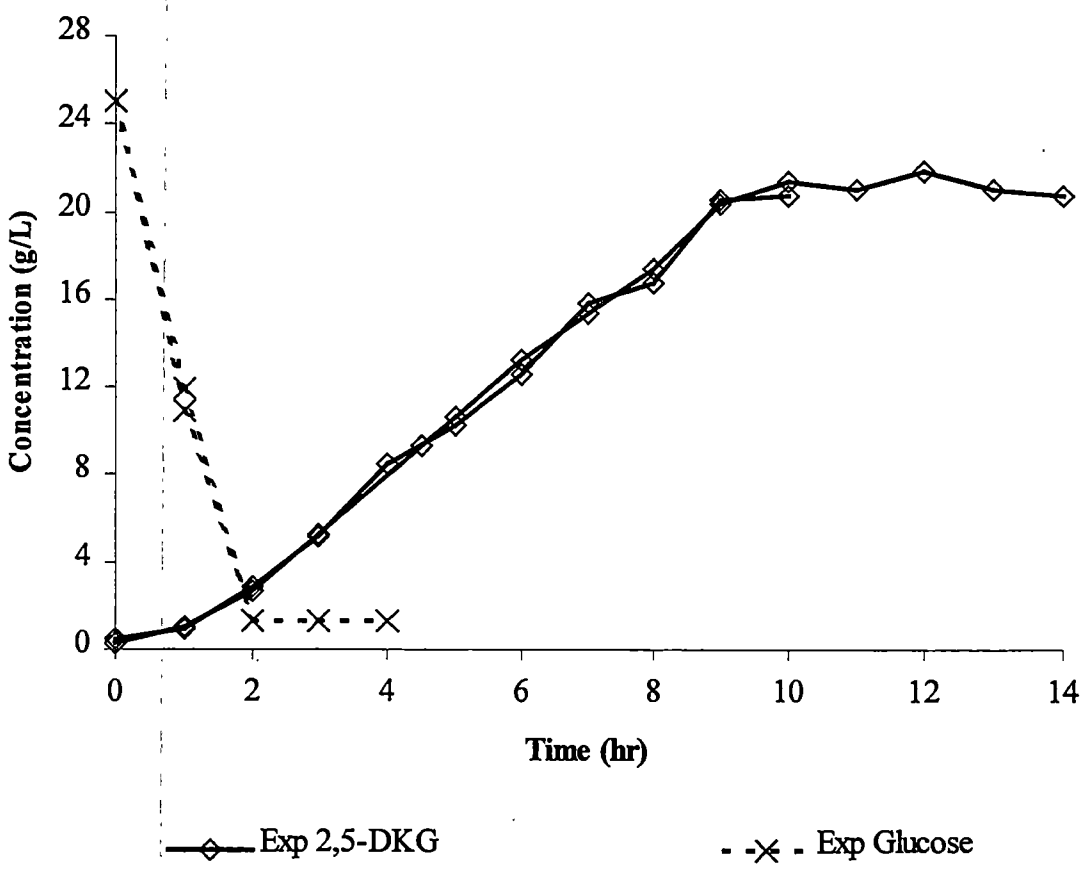


Figure 6-3 Glucose and 2,5-DKG concentration profiles in batch experiments using whole cells (volumetric 2-KDG dehydrogenase activity = 15.95 U/mL)

experiments yielded nearly identical results. In both cases, the concentration of 2,5-DKG stopped increasing after 9 hours. The rate of change in 2,5-DKG concentration was very slow in the first 2 hours, but quickly increased thereafter. The 2,5-DKG concentration appeared to increase linearly over time for the next 7 hours. The final concentration of 2,5-DKG in the reactor in the two cases after 9 hours was 21.15 ± 0.45 g/L. The total conversions from 25 g/L of glucose obtained in both cases were 71% and 76%. All of the substrate glucose in both cases was consumed after 2 hours.

Figure 6-4 shows the reactor concentration of glucose and 2,5-DKG over time in the two experiments conducted at the higher cell concentration. The overall shape of the profiles was similar to those in the lower cell concentration experiments. The concentration of 2,5-DKG stopped increasing after 7 hours, 2 hours less than the time observed in the lower cell density experiment. The final concentration of 2,5-DKG in the reactor in both cases after 7 hours was 20 ± 0.55 g/L. The total conversions from 25 g/L of glucose obtained in the two cases were 77 % and 74 %, or 75.5 ± 1.5 %. As in the previous experiment, all of the substrate glucose was consumed after 2 hours. Increasing the amount of cells in the reactor resulted in no increase in overall conversion. The only change resulting from increasing the cell concentrations in the reactor was the shortened amount of time required to reach the final conversion.

6.4.2 Batch production of 2,5-DKG using French-pressed *P. citrea* cells

Results from the batch 2,5-DKG production experiment indicated that approximately 25 % of glucose was not converted to 2,5-DKG. The amount of glucose

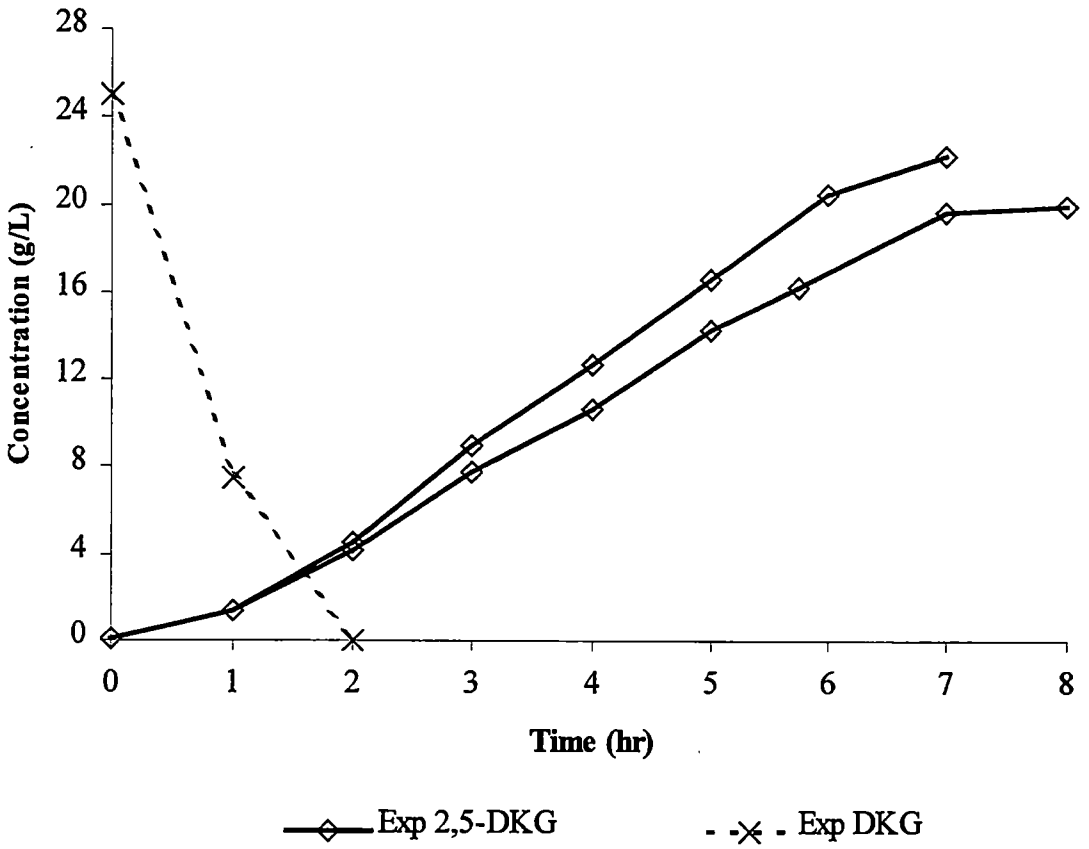


Figure 6-4 Glucose and 2,5-DKG concentration profiles in batch experiments using whole cells (volumetric 2-KDG dehydrogenase = 24.6 U/mL)

not converted may be channeled down into the other pathways associated with central metabolism listed in Table 3-1. This hypothesis was tested by performing similar batch production experiments using nonviable forms of *P. citrea* in which central metabolism was eliminated by cellular lysis and using only the cell membrane fraction. By performing the batch experiments using only the membrane fraction, degradation of glucose by central metabolism should be eliminated from the reactor, and the overall conversion from glucose to 2,5-DKG should be near 100%.

Lysis was achieved by passing the cells through a French press. This allows the separation of membrane fractions and intracellular materials by ultracentrifugation. Two experiments were performed, and Figure 6-5 shows the glucose and 2,5-DKG concentrations over time. The overall shape of the experimental 2,5-DKG concentration profile over time resembled that of the experiments with whole cells. The two experiments conducted yielded nearly identical results. The concentration of 2,5-DKG stopped increasing after 12 hours, and remained at 20.47 ± 0.15 g/L. The two batch productions resulted in overall conversions to 2,5-DKG of 71.1 % and 71.6 % or 71.35 ± 0.25 %. As in the previous experiments performed with whole cells, all of the substrate glucose in both cases was consumed after 2 hours. 2-KDG dehydrogenase enzyme assay was performed on samples taken from the beginning and end of both experiments. 2-KDG dehydrogenase was found to have a higher volumetric activity in the French-pressed cells than in whole cells. By losing all of the intracellular content as a result of the lysis process, the cell itself has undergone a tremendous volume reduction. Thus, for a unit volume, there was now more membrane and subsequently more 2-KDG

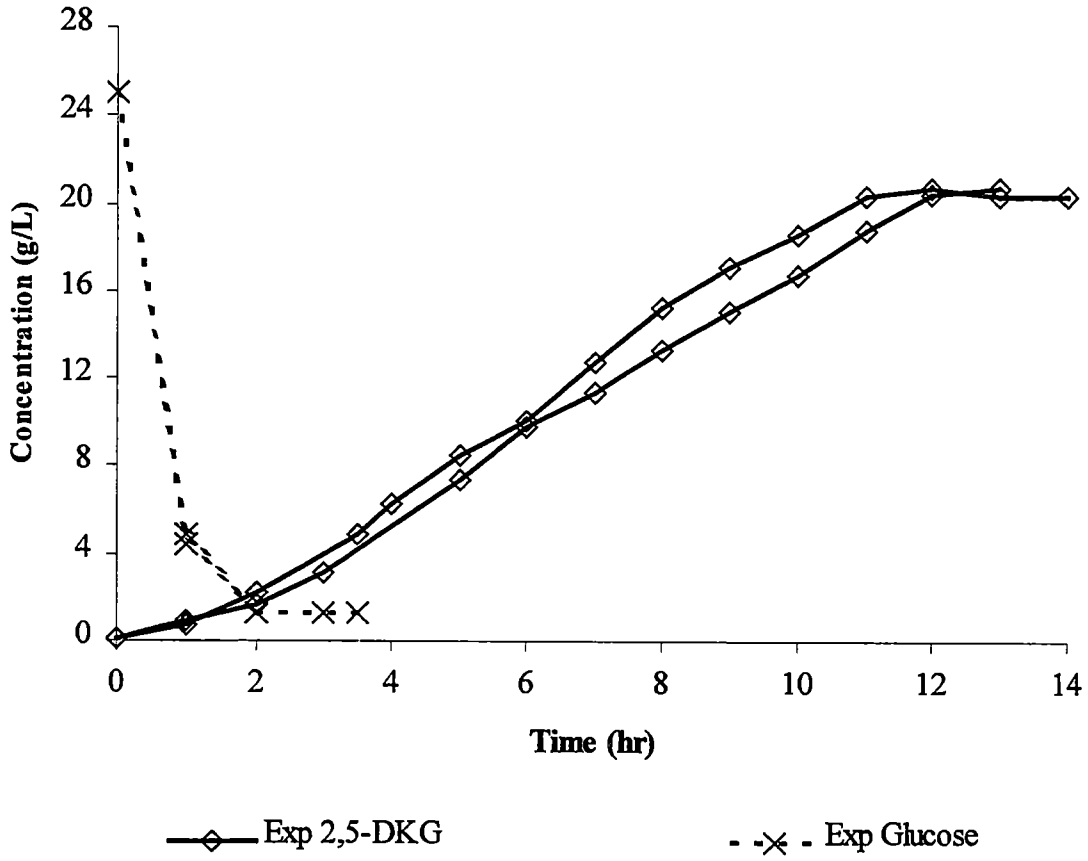


Figure 6-5 Glucose and 2,5-DKG concentration profiles in batch experiments using French-pressed cells (volumetric 2-KDG dehydrogenase activity = 19.05 U/mL)

dehydrogenase, in the French-pressed cells than in whole cells. Volumetric 2-KDG dehydrogenase enzyme activity did not decrease over the period of both experiments (Table 6-6). Total protein concentration also remained fairly constant.

Table 6-6 Volumetric 2-KDG Dehydrogenase Enzyme Activity and Protein Concentration at the Beginning and End of Batch Production of 2,5-DKG Using French-pressed Cells

	T = 0 hr	T = 14 hr
Volumetric Activity (U/ml)	19.05 ± 0.35	18.44 ± 0.61
Protein Concentration (mg/ml)	0.49 ± 0.028	0.57 ± 0.045
Specific activity (U/mg)	39.03 ± 0.71	32.56 ± 1.07

Surprisingly, the glucose conversion for French-pressed cells (approximately 71 %) was not higher than that for whole cells (approximately 75 %). One reason may be that French pressing the cells was not an adequate method of cellular lysis. Samples from the two French-pressed cell experiments were plated onto LB rich plates and allowed to incubate at 37 °C overnight. Whole cells were also plated as a reference. Colonies of viable cells were formed on the LB plates innoculated with French-pressed cells. However, visual inspection indicated that the number of colonies formed was somewhat less than those formed on plates innoculated with viable whole cells, suggesting that while 100% cellular lysis was not achieved, some cellular lysis did occur.

The rate of formation of 2,5-DKG was also observed to be slower than in the whole cell case. The concentration of 2,5-DKG stopped increasing after 12 hour, 2 hours longer than in the lower concentration whole cell case. The volumetric enzyme activity

measured (19.05 U/ml), however, was higher than that measured in the whole cell case (15.95 U/ml). With an increased volumetric activity, the rate of formation of 2,5-DKG was hypothesized to increase as well.

This apparent contradiction may partially be explained by examining the French pressing process itself and its effect on the membrane-bound enzymes. Figure 6-6 shows a cross section schematic of a French press cell chamber. The French press chamber consisted of a stainless steel cylinder fitted with a plunger inserted from one end. The other end of the cylinder contains a removable base, above which a small orifice is located in the cylinder wall connecting the inside of the chamber to the outside. A needle valve controls the flowrate through this aperture. Upon pressure drop (15,000 psi) as a cell suspension passes through the orifice, and the cellular membranes are disrupted by hydrodynamic shear. The effect of this hydrodynamic shear on the integrity of the enzymes bound to the membrane is unclear and merits further investigation.

6.4.3 Batch production of 2,5-DKG using permeabilized *P. citrea* cells

Another common technique to render cells nonviable is the permeabilization of the cellular membrane with an organic solvent. By chemically treating the cells with a permeabilizing agent, the cell membrane is rendered permeable to large molecular weight compounds by means of simple diffusion. The intracellular material also become susceptible to simple diffusion across the membrane. Central metabolic pathways, especially oxidative phosphorylation, which depend heavily upon the selectivity and"intactness" of the membrane, are rendered nonfunctional upon permeabilization

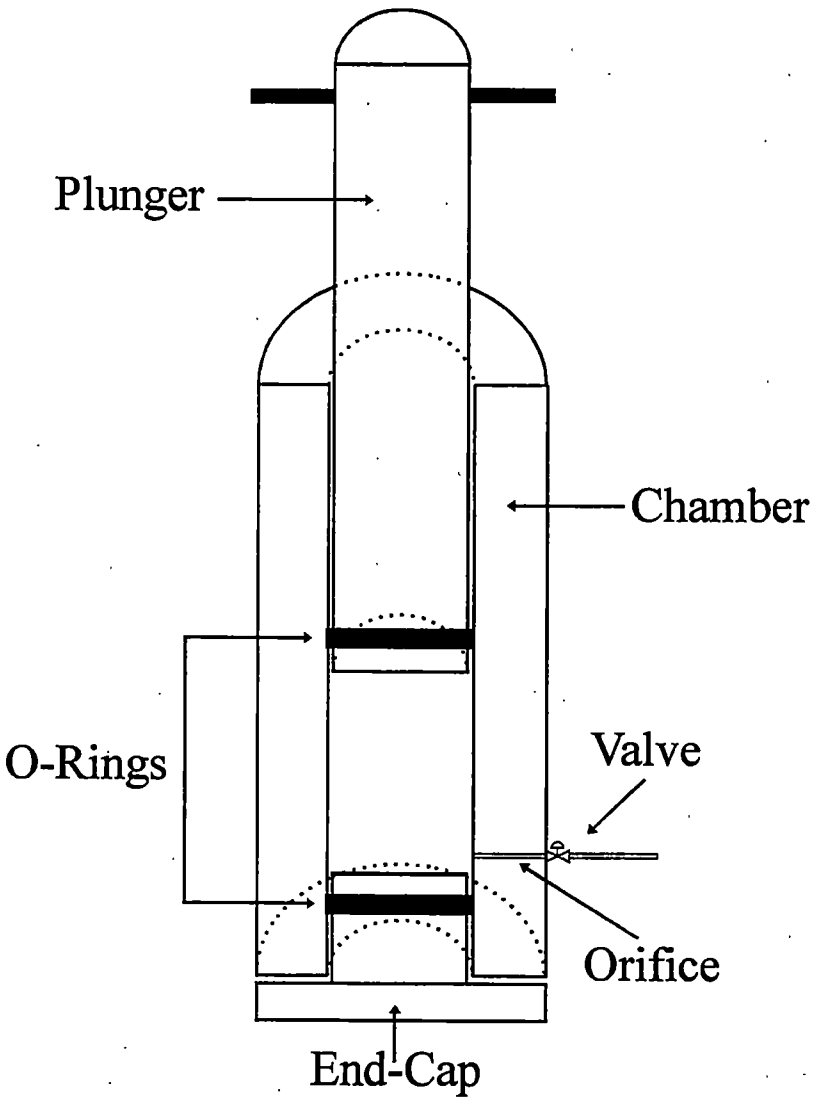


Figure 6-6 Cross section schematic of a French press cell chamber

of the membrane. The permeabilization method discussed previously in Section 4.7.2 used toluene as the permeabilizing agent (Boston, 1999). The exact mechanism by which toluene causes permeabilization of the membrane is not clear; however, the target is probably the lipid regions of the membrane (Gerhardt, 1994).

Two batch experiments were performed using permeabilized cells. The experimental conditions were similar to those in experiments performed with whole cells and French-pressed cells. Figure 6-7 shows the glucose and 2,5-DKG concentrations over time. In both experiments, 2,5-DKG stopped increasing after 17 hours, and remained at 25.27 ± 0.31 g/L. The two batch productions resulted in overall conversions to 2,5-DKG of 90% and 92%. All of the substrate glucose in both cases was consumed after 2 hours. 2-KDG dehydrogenase enzyme assay was performed on samples taken from the beginning and end of both experiments. The volumetric activity of 2-KDG dehydrogenase was fairly constant over the period of both experiments (Table 6-7). Total protein concentration also remained approximately constant.

Table 6-7 Volumetric 2-KDG Dehydrogenase Enzyme Activity and Protein Concentration at the Beginning and End of Batch Production of 2,5-DKG Using Permeabilized Cells

	T = 0 hr	T = 14 hr
Volumetric Activity (U/ml)	22.43 ± 0.59	29.38 ± 0.07
Protein Concentration (mg/ml)	0.53 ± 0.085	0.36 ± 0.041
Specific activity (U/mg)	87.59 ± 2.36	80.53 ± 0.20

Unlike the results from experiments using French-pressed cells, the results from the experiments using permeabilized cells did help reinforce the hypothesis that elimination of central metabolism would increase the overall conversion of glucose to

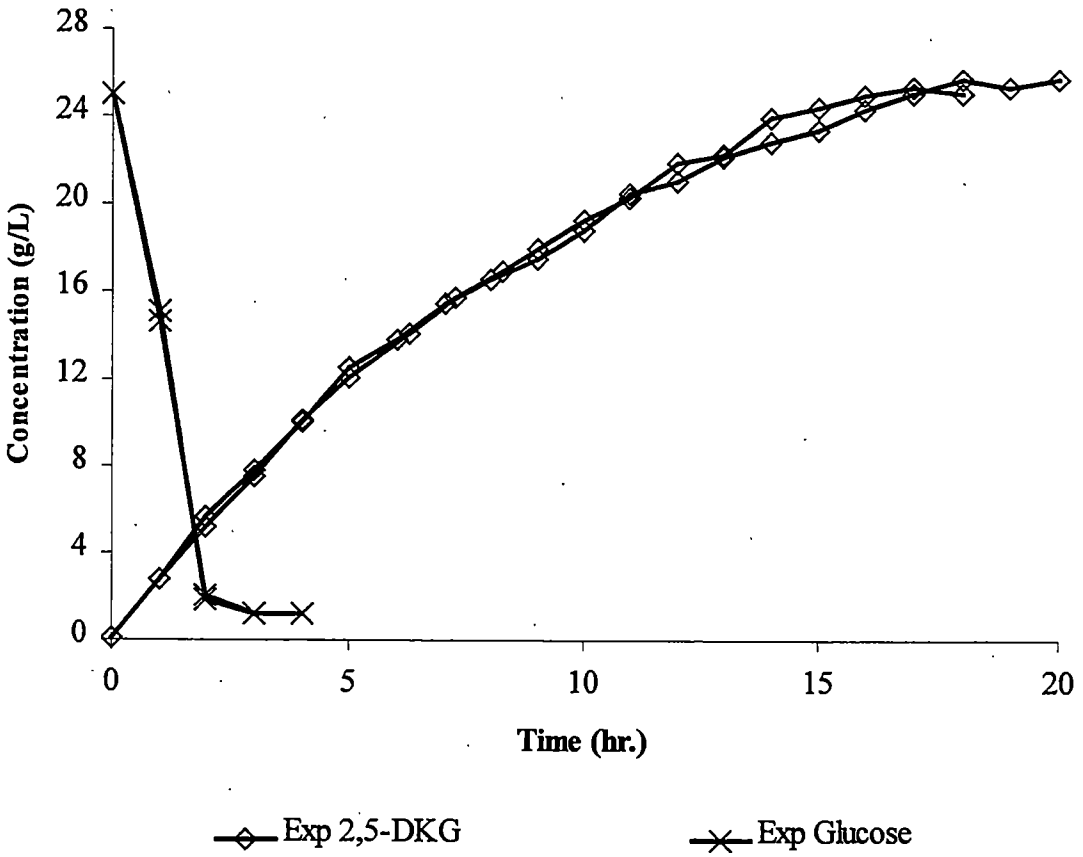


Figure 6-7 Glucose and 2,5-DKG concentration profiles in batch experiments using permeabilized cells (volumetric 2-KDG dehydrogenase activity = 22.43 U/mL)

2,5-DKG. The conversion in this case was 91%, a definite increase from the 75 % obtained from the whole cell case. The total glucose that was unaccounted for (9%) may, like in the French-pressed cell case, be attributed to the presence of central metabolism. Samples from permeabilized cell experiments were plated onto LB rich plates and incubated at 37 °C overnight. Whole cells were also plated as a reference. Like the plates innoculated with French-pressed cells, the plates innoculated with permeabilized cells also had colony formations. However, the number of colonies formed was somewhat less than those formed on plates innoculated with viable whole cells, indicating that of the permeabilized cells used for the batch experiment, a portion remained viable and able to utilize glucose for central metabolism.

The time taken for the 2,5-DKG concentration to stabilize, 17 hours, was observed to be considerably longer than the 7 hours it took in the whole cell case. The overall shape of the 2,5-DKG concentration profile in Figure 6-7 did not resemble that of the experiments with whole cells (Figure 6-3 and Figure 6-4) or French-pressed cells (Figure 6-5). The overall shape of the 2,5-DKG concentration profile was no longer sigmoidal but hyperbolic. This saturational shape was observed in both batch experiments conducted with permeabilized cells. The difference in the shapes of 2,5-DKG profile may be indicative fundamental changes in the enzymes themselves. For example, allosteric enzymes do not obey Michaelis-Menten kinetics (Stryer, 1995). Allosteric enzymes often display sigmoidal plots of the reaction velocity V versus substrate concentration [S] (See Figure 6-8). In allosteric enzymes, the binding of substrate to one active site can affect the binding properties of other active sites in the

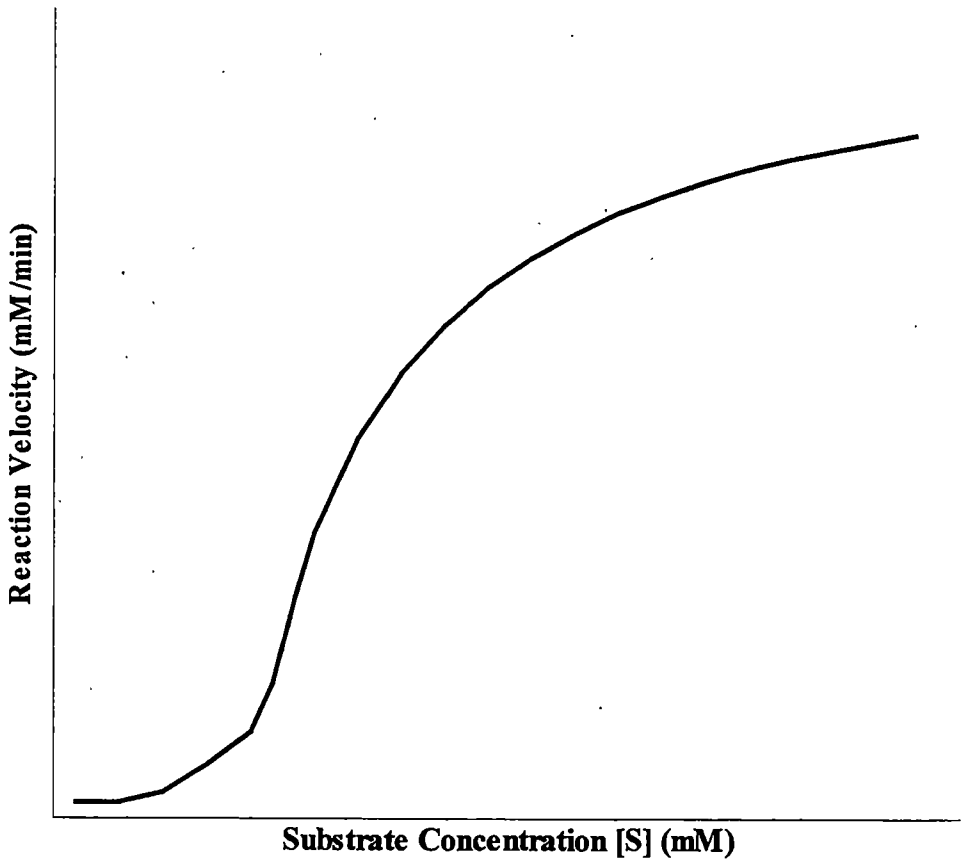


Figure 6-8 Sigmoidal dependence of reaction velocity on substrate concentration [S] for an allosteric enzyme

same enzyme molecule. A possible outcome of this interaction between subunits is that the binding of substrate becomes cooperative, which would give a sigmoidal shape to the plot of V versus [S]. For Michaelis-Menten enzymes, binding of the substrate to one active site does not affect the binding properties of other active sites. Thus the plot of V versus [S] takes a hyperbolic shape (Stryer, 1995).

The change in the shape of the 2,5-DKG concentration profile may be attributed to the chemical treatment of the membrane-bound enzymes in the permeabilization procedure. Though the effect of toluene on cellular membrane and the bound enzymes are unknown, a definite difference in the overall shape of the 2,5-DKG profiles as well as rate of conversion (17 hours with permeabilized cells versus the 7 hours for the whole cells) were observed in experiments conducted with permeabilized cells.

7 Mathematical Modeling of 2,5-DKG Concentration Profile

The mathematical model developed was used to predict the 2,5-DKG concentration profiles in the batch case. The model consists of Equations 5.1 - 5.4. To solve the model equations, the following physical inputs are needed:

- The volumetric activity of glucose dehydrogenase (E1) in U/ml
- The volumetric activity of gluconate dehydrogenase (E2) in U/ml
- The volumetric activity of 2-KDG dehydrogenase (E3) in U/ml
- The maximum specific glucose uptake rate constant U_T in mmole of glucose/min/g (dw) of cells
- The concentration of cells (X) in g dry weight /L
- The half saturation constant $\left(K_M^{U_i}\right)$ in mM

Of the volumetric activities, only the volumetric E3 activity was measured. The assay procedures for measuring volumetric E1 and E2 activities presented in Sections 4.5.1 and 4.5.2 only work for purified enzymes and would not work for *P. citrea* due to the fact that *P. citrea* has all three enzymes present. Ferricyanide was used in all three assays as the electron acceptor. The product of the reaction catalyzed by E1 serves as the substrate in the reaction catalyzed by E2. The product of the reaction catalyzed by E2 serves as the substrate in the reaction catalyzed by E3. In an assay for the E1 activity, the ferricyanide would be consumed by three parallel reactions in stead of the reaction of choice. Only the E3 activity is assayed because the product of the reaction catalyzed by E3 will not be the substrate in any other reactions. Since there are no good ways to quantify the volumetric activities of E1 and E2, and U_T, they have to be determined by fitting experimental data.

The concentration of cells ([X]) was determined by measuring the absorbance at 600 nm of the reactor broth diluted tenfold. The absorbance reading (between 0.1 and 1) was converted to g dry weight/mL by the equation in Figure 6-1. The half saturation constant $\left(K_M^{U_i}\right)$ in mM was set to be infinitely small as explained in Section 5.1.1.

7.1 Modeling 2,5-DKG Concentration in the Whole Cell Batch Experiment (the Low Concentration Case)

The volumetric E3 activity in the low cell concentration whole cell batch experiment was determined to be 15.95 U/ml. The cell density is calculated by using the dry weight and OD correlation shown in Figure 6-1. The absorbance at 600 nm taken of the 1 to 10 dilution of reactor broths was 0.5 (Table 6-5). The dry weight concentration of the cell was determined to be 2.71 g/L.

Values of the volumetric E1 and E2 activities, and U_T were fit by the trial and error procedure discussed below. Using volumetric E1 activity = volumetric E2 activity = volumetric E3 activity = 15.95 U/ml and U_T = 0.08 mmol/g/min, the model was able to give a very good fit of the experimental 2,5-DKG profiles (Figure 7-1).

A sensitivity analysis was performed to determine whether changes in the model parameters had a significant effect on both the overall conversion of glucose to 2,5-DKG and the rate of 2,5-DKG formation. Each parameter was varied while holding other parameters constant at the corresponding nominal value. The nominal value for both volumetric E1 and E2 activities is 15.95 U/ml, and for U_T is 0.08 mmol/g/min. The

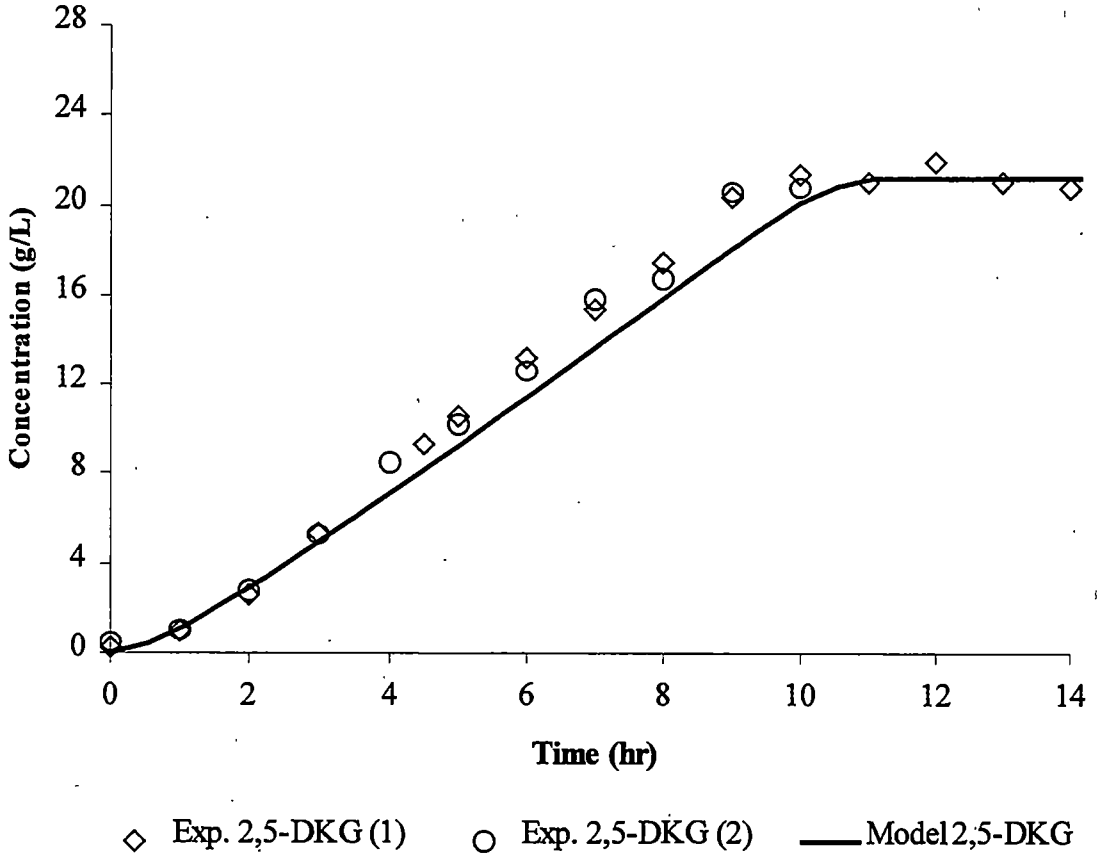


Figure 7-1 Experimental 2,5-DKG concentration profiles from batch experiment using whole cells and model fit using parameters: volumetric E1 activity = volumetric E2 activity = volumetric E3 activity = 19.45 U/mL, and U_T = 0.08 mmol/g/min

overall conversion of glucose to 2,5-DKG was 79.2 %, and the amount of time taken to reach the maximum conversion was 11 hours.

7.1.1 Sensitivity Analysis for the Model Parameter Volumetric E1 Activity

The effect of varying the volumetric E1 activity around the nominal value of 15.95 U/mL on the 2,5-DKG concentration profile is shown in Figure 7-2. The effect was studied for both small and large perturbations of volumetric E1 activity. Values of the volumetric E1 activity used were: 1.2, 0.8, 10, 0.1 times E1 nominal volumetric activity, and infinity. Increasing the volumetric E1 activity had virtually no effect on the time required to reach the nominal case maximum conversion of 79%, although it did affect the maximum conversion reached. This indicates that the volumetric E1 activity was not kinetically rate limiting in the production of 2,5-DKG. However, the overall conversion of glucose to 2,5-DKG was increased as a result of increasing the volumetric E1 activity. When the volumetric E1 activity was infinite, the conversion was 100%. Since there was more E1 present, glucose was channeled down the 2,5-DKG pathway at a faster rate, and the amount of glucose channeled down central metabolism was decreased. Hence, the increase in overall conversion was observed. Decreasing the volumetric E1 activity slightly (-20%) shows a small loss in overall conversion (from 79.2 % down to 75.4%). Nominal case conversion was never achieved, but the time required for 75.4% conversion was approximately 10 hours. Decreasing the volumetric E1 activity by 10 fold resulted in drastically different results. In this case, the amount of E1 had become so small, resulting in much less glucose been channeled down the 2,5-DKG pathway and a much smaller conversion (30%). Consequently, more glucose was available to be

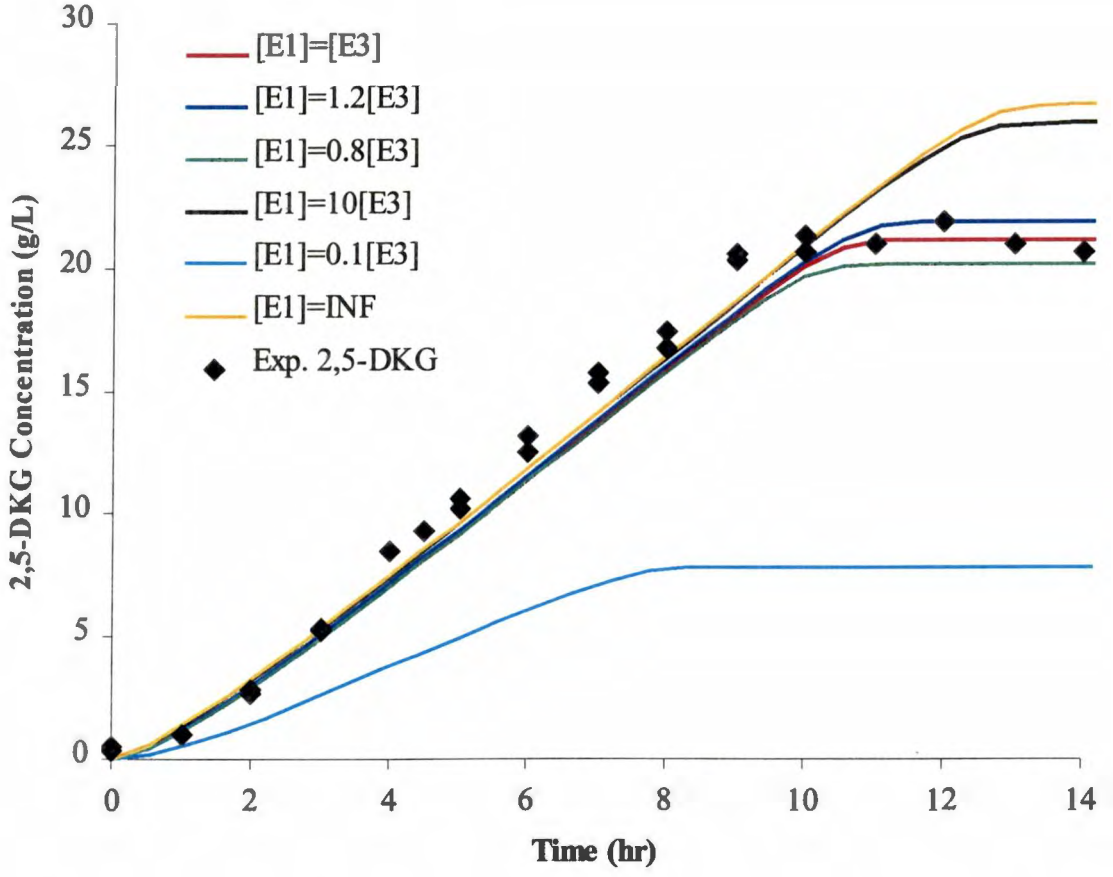


Figure 7-2 The effects of perturbations in the volumetric E1 activity on the overall conversion of glucose to 2,5-DKG and the time required to reach nominal conversion of 79%

channeled down central metabolism. The 2,5-DKG was limited by the amount of E1. The results of these perturbations of E1 activity are summarized in Table 7-1.

Table 7-1 Result of Perturbation of the Volumetric Glucose Dehydrogenase (E1) Activity on the Overall Conversion of Glucose to 2,5-DKG and Time Required for Nominal Conversion

Volumetric E1 Activity (U/ml)	Overall Conversion (%)	Time Required for Nominal Conversion (hr.)
$E1_{nom}$ = 15.95	79	11
1.2 $E1_{nom}$ (+20%)	82	11
10 $E1_{nom}$ (+10 fold)	97	11
Infinity	100	11
0.8 $E1_{nom}$ (-20%)	76	10
0.1 $E1_{nom}$ (-10 fold)	29	-

7.1.2 Sensitivity Analysis for the Model Parameter E2 Activity

The effect of changing the volumetric E2 activity on the 2,5-DKG concentration profile is shown in Figure 7-3. The effect was observed for both small and large perturbations of the volumetric E2 activity. Values of the volumetric E2 activity used were: 1.2, 0.8, 10, and 0.1 times E2 volumetric activity nominal (15.95 U/ml), and infinity. Increasing the volumetric E2 activity had no effect on the overall conversion of glucose to 2,5-DKG. Since cellular uptake of gluconate was not modeled, all the gluconate formed from the first reaction (catalyzed by E1) was converted to 2,5-DKG. Increasing the volumetric E2 activity does however affect the time required for nominal case maximum conversion, 79.2%. A 20% increase in the volumetric E2 activity resulted in 1 hour reduction in time required to reach 79.2 % conversion, which was 11 hr. A 10-

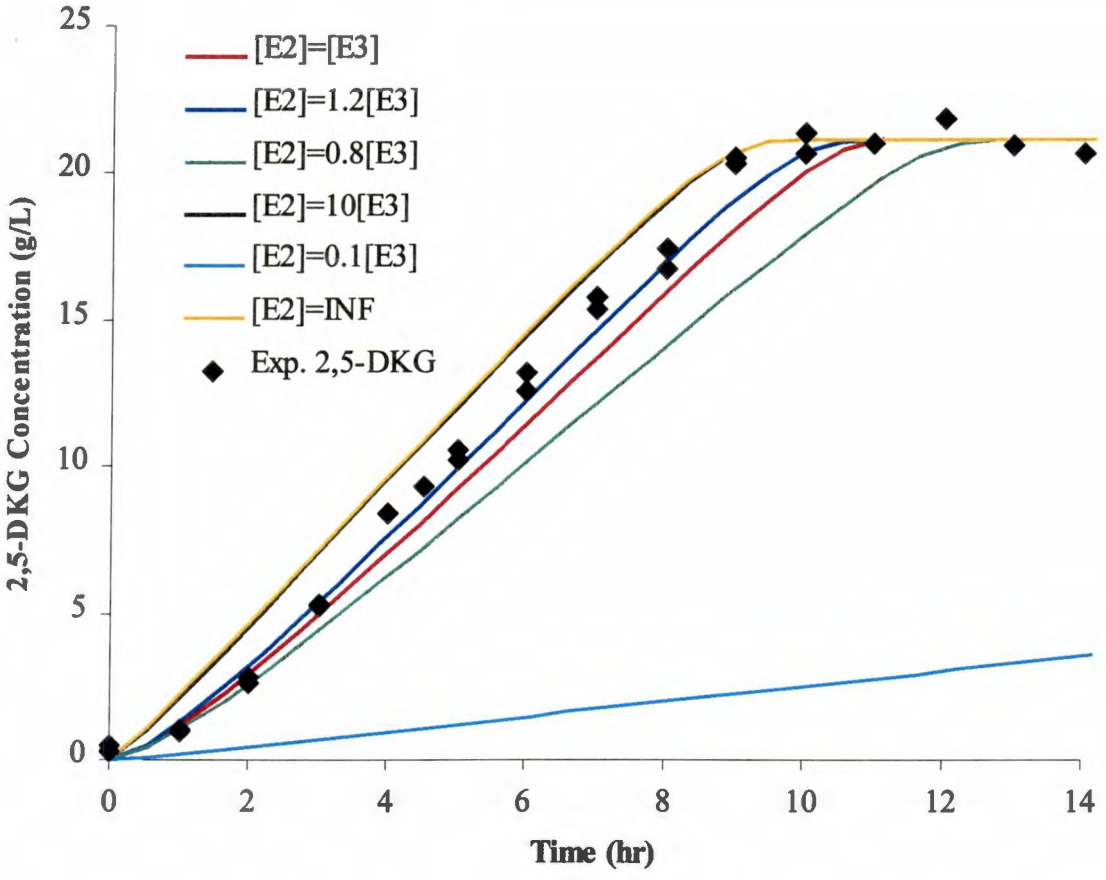


Figure 7-3 The effects of perturbations in the volumetric E2 activity on the overall conversion of glucose to 2,5-DKG and the time required to reach nominal conversion of 79%

fold increase in E2 activity resulted in 2 hours reduction to reach 79.2%. An increase of E2 activity to infinity resulted also in 2 hours reduction. This indicated that E2 may be kinetically rate limiting in the 2,5-DKG pathway. Increasing the volumetric E2 activity resulted in a reduction in time to reach the nominal conversion. Decreasing the volumetric E2 activity by 20% resulted in 1 hours increase for the nominal conversion time. A 10-fold decrease in the volumetric E2 activity resulted in a 15% overall conversion in 10 hours. 2,5-DKG production was rate limited by the amount of E2 present. The results of these perturbations of the volumetric E2 activity are summarized in Table 7-1

Table 7-2 Result of Perturbation of Gluconate dehydrogenase (E2) Activity on the Conversion of Glucose to 2,5-DKG and Time Required for Nominal Conversion

E2 Activity (U/ml)	Overall Conversion (%)	Time Required for Nominal Conversion (hr.)
$E2_{nom}$ = 15.95	79	11
1.2 $E2_{nom}$ (+20%)	79	10.5
10 $E2_{nom}$ (+10 fold)	79	9.5
Infinity	79	9.5
0.8 $E2_{nom}$ (-20%)	79	12
0.1 $E2_{nom}$ (-10 fold)	15	-

7.1.3 Sensitivity Analysis for the Model Parameter U_T

The amount of glucose diverted to central metabolism, dictated by U_T, does not affect the rate of production of 2,5-DKG. Only the overall conversion of glucose to 2,5-DKG is affected by U_T. The smaller the value of U_T, the less glucose is directed to central metabolism, and thus a higher conversion to 2,5-DKG. The effect of changing U_T

on the 2,5-DKG concentration profile is shown in Figure 7-4. The effect was observed for both small and large perturbations of U_T. Values of U_T used were: 1.2, 0.8, 10, and 0.1 times U_T nominal (0.08 mmol/g/min), and 0. Decreasing U_T had virtually no effect on the time required to reach nominal conversion of 79%. When U_T was 0, the conversion was of course 100%. Increasing U_T slightly (+20% of its nominal value) showed a small loss in overall conversion (from 79.2 % in the nominal case down to 76.2%). Nominal case conversion was never achieved, but the time required for 76.2% conversion was 10 hours. Increasing U_T by 10 fold resulted in drastically different results. In this case, the uptake rate of glucose had become so great, resulting in much less glucose been channeled down the 2,5-DKG pathway and hence a much smaller conversion (31 %). The results of these perturbations of U_T are summarized in Table 7-3.

Table 7-3 Result of Perturbation of Glucose Uptake Rate Constant (U_T) on the Overall Conversion of Glucose to 2,5-DKG and Time Required for Nominal Conversion

U_T (mmol/g/min)	Overall Conversion (%)	Time Required for Nominal Conversion (hr.)
$U_{T,nom} = 0.08$	79	11
1.2 $U_{T,nom}$ (+20%)	76	10
10 $U_{T,nom}$ (+10 fold)	29	-
0	100	11
0.8 $U_{T,nom}$ (-20%)	83	11
0.1 $U_{T,nom}$ (-10 fold)	97	11

In summary, the sensitivity analysis performed revealed that small (±20%) perturbations of the volumetric E1 and E2 activities, and U_T did not affect greatly either

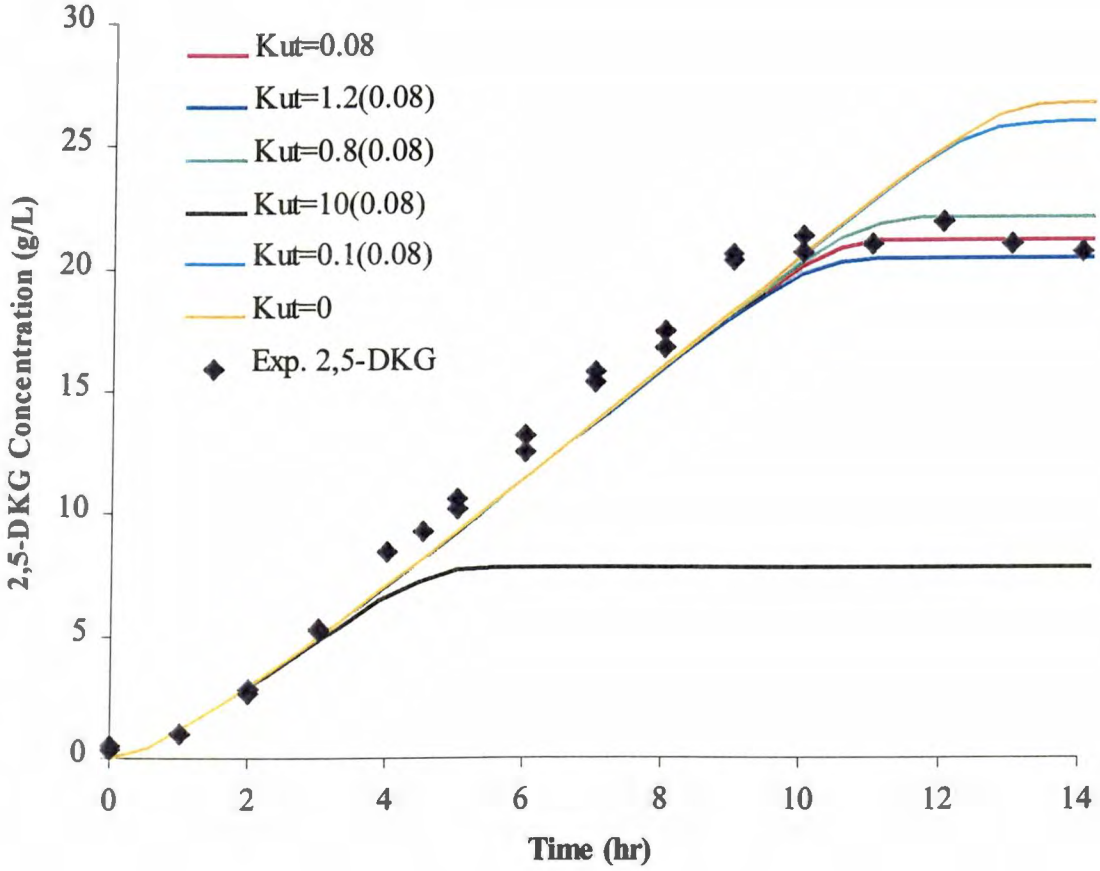


Figure 7-4 The effects of perturbations in U_T (in mmol/g/min)on the overall conversion of glucose to 2,5-DKG and the time required to reach nominal conversion of 79%

the overall conversion of glucose to 2,5-DKG nor the time required to achieve that conversion. The nominal conversion was most sensitive to perturbations in the volumetric E1 activity and U_T, and the time required to achieve the nominal conversion was most sensitive to the perturbations in the volumetric E2 activity.

7.2 Modeling 2,5-DKG Concentration in the Whole Cell Batch Experiment (High Cell Concentration)

Using values of the volumetric E1 and E2 activities chosen to be the same as the volumetric E3 activity, and a fit U_T value of 0.08 mmol/g/min, the model predicted the experimental results very well in the low concentration whole cell batch experiments. As discussed in section 7.1, a sensitivity analysis revealed that the model results for 2,5-DKG concentration profile were not significantly affected by small (±20%) changes in the values of the volumetric E1 and E2 activities and U_T. The model was tested again through application to another set of whole cell batch experimental results at a higher cell concentration.

The volumetric E3 activity in the high cell concentration whole cell batch experiment was experimentally determined to be 24.6 U/ml, compared to 15.95 U/ml in the lower concentration experiment. Using the volumetric E1 activity = the volumetric E2 activity = the volumetric E3 activity = 24.6 U/ml and U_T = 0.08 mmol/g/min, the model was able to give a very good fit of the experimental 2,5-DKG profiles (Figure 7-5). The experimental data showed a 75% conversion in 7 hour. The model predicted a 76 % conversion in approximately 7 hours.

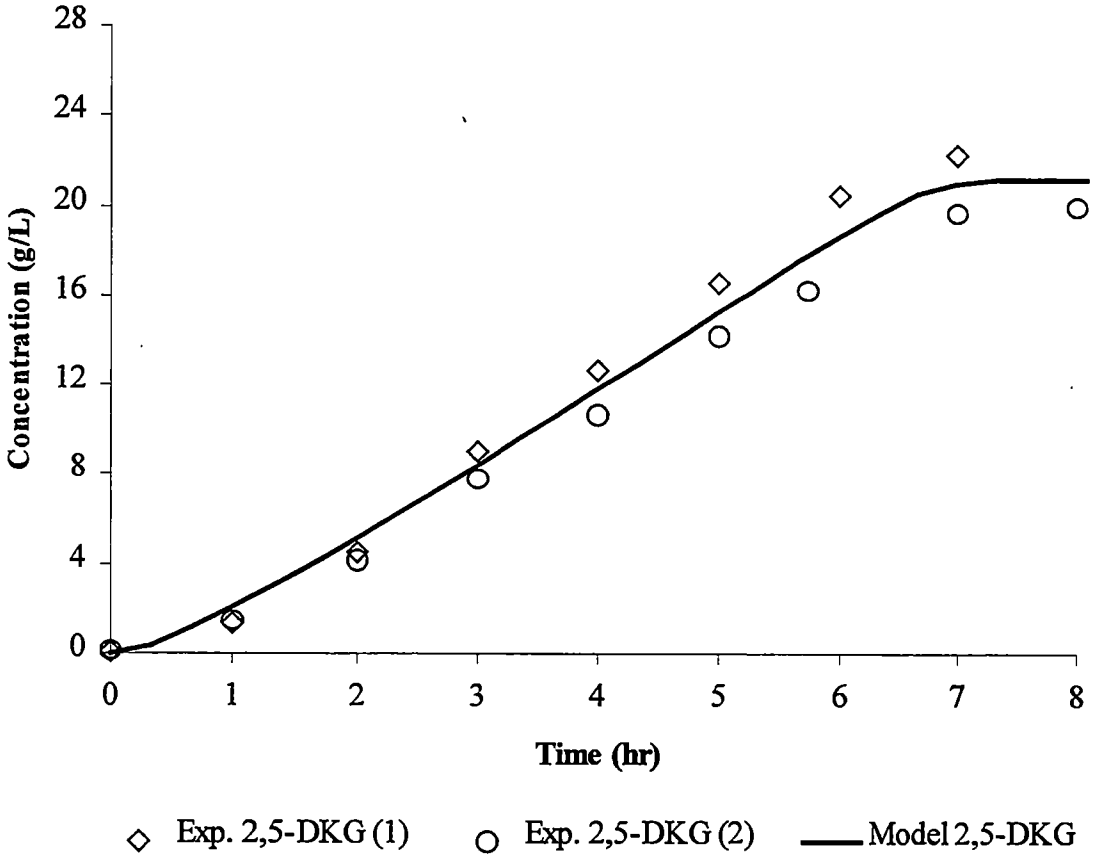


Figure 7-5 Experimental 2,5-DKG concentration profiles from batch experiment using whole cells and model fit using parameters: volumetric E1 activity = volumetric E2 activity = volumetric E3 activity = 24.6 U/mL, and U_T = 0.08 mmol/g/min

7.3 Modeling 2,5-DKG Concentration in Batch Experiments Using Nonviable Cells

Figure 7-6 shows both the predicted and experimental 2,5-DKG concentration profiles for the batch experiments performed with French-pressed cells using the values of the volumetric E1 and E2 activities chosen to be the same as the volumetric E3 activity (19.05 U/ml). The model predicted 100% conversion of glucose to 2,5-DKG in 10.5 hours. However, the experimental results indicate a 71% conversion in 11 hours. Figure 7-7 shows both the predicted and experimental 2,5-DKG concentration profiles for the batch experiments performed with permeabilized cells using the values of the volumetric E1 and E2 activities to be the same as the volumetric E3 activity (22.43 U/ml). The model predicted 100% conversion of glucose to 2,5-DKG in 9 hours. However, the experimental results indicate a 91 % conversion in 18 hours.

The model was not able to predict the experimental results very well in the batch experiments performed with French-pressed or permeabilized cells. The parameter U_T was set to zero in modeling experiments using nonviable cells because of the assumption of the absence of central metabolism. However, as previously discussed in Sections 6.4.2 and 6.4.3, this assumption was not valid. In addition, the overall shape of the experimental and model profiles were different; the experimental profile was hyperbolic, and the model profile was sigmoidal. The exact effect of the processes used to render the cells nonviable on the membrane enzymes themselves was unclear, but changes have been observed. Until these effects are elucidated and incorporated into the mathematical

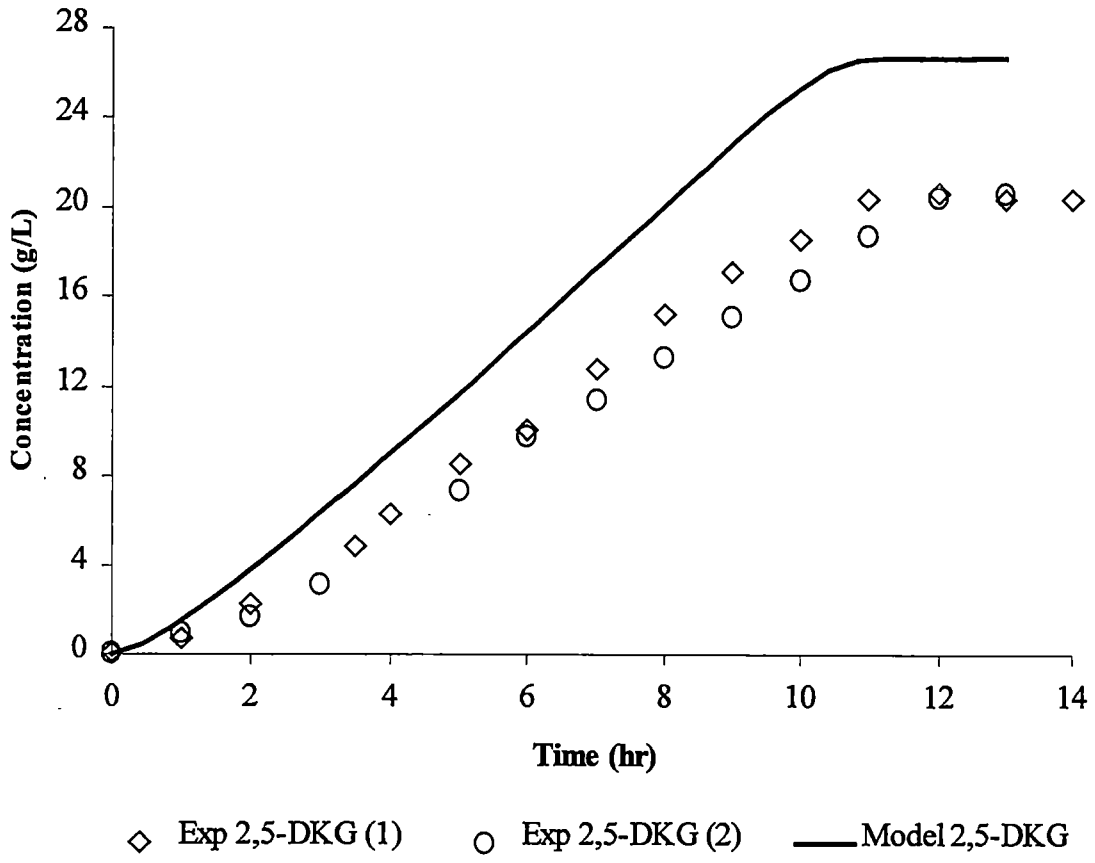


Figure 7-6 Experimental 2,5-DKG concentration profiles from batch experiment using French-pressed cells and model fit using parameters: volumetric E1 activity = volumetric E2 activity = volumetric E3 activity = 19.05 U/mL, and $U_T = 0$ mmol/g/min

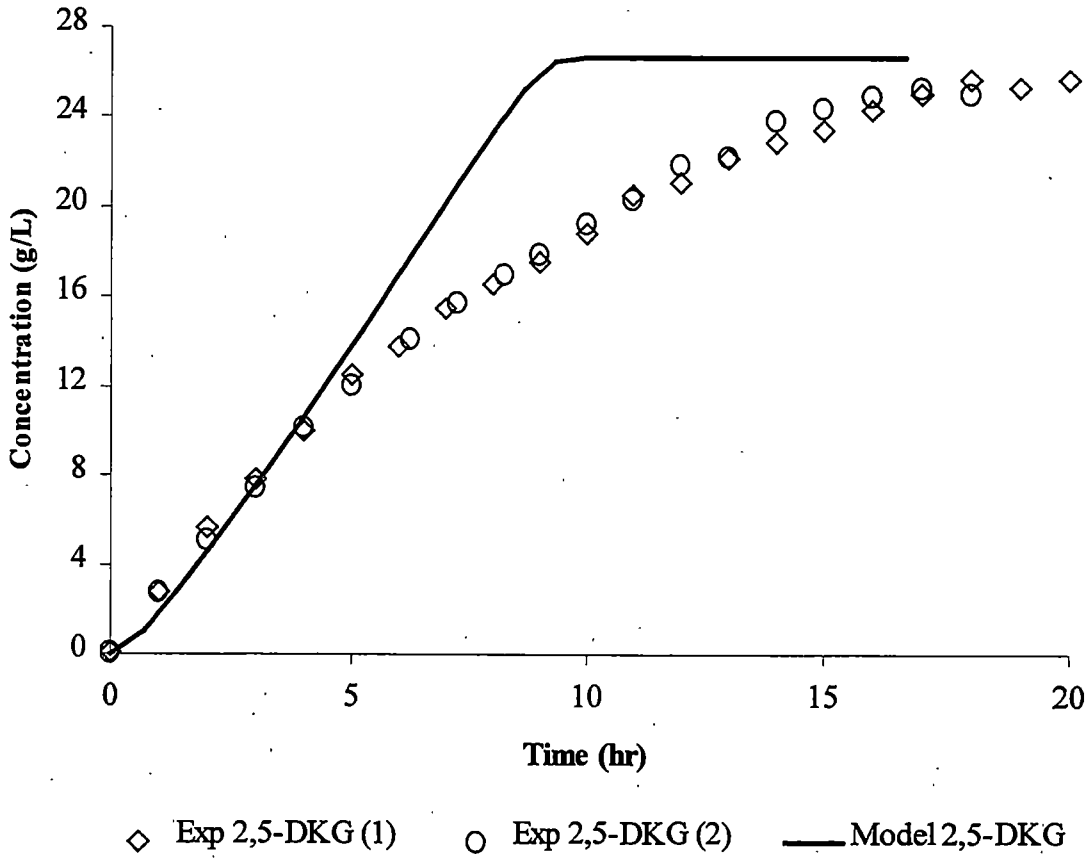


Figure 7-7 Experimental 2,5-DKG concentration profiles from batch experiment using permeabilized cells and model fit using parameters: volumetric E1 activity = volumetric E2 activity = volumetric E3 activity = 22.43 U/mL, and $U_T = 0$ mmol/g/min

model, the present model does not predict adequately the 2,5-DKG profiles in batch production using nonviable cells.

8 Conclusions

The experimental and mathematical analyses performed in the batch production of 2,5-DKG using *Pantoea citrea* were motivated by the following objectives: (a) determine the degree to which central metabolism effects glucose utilization in the batch production of 2,5-DKG in both viable and nonviable *P. citrea* cells, (b) develop a mathematical model for 2,5-DKG batch production that accounts for glucose utilization by the enzymes responsible for 2,5-DKG production and by central metabolism, and (c) validate the mathematical model by applying it to various cases of batch production using both viable and nonviable cells.

Based on maximum growth rate and substrate yield, glucose was a poor growth substrate (μ_{max}=0.15 hr^{-1} and Y_{sub}=0.089 g dw/g sub. respectively) while fructose was the best substrate (μ_{max}=4.25 hr^{-1} and Y_{sub}=0.17 g dw/g respectively). The substrate yields for fructose and gluconate were equivalent (Y_{sub}=0.17 g dw/g) while the maximum growth rates were 4.25 hr^{-1} and 1.01 hr^{-1}, respectively. Internal enzyme activity measurements showed that the pentose phosphate pathway had a higher activity than the Entner-Douderoff and Embden-Mayerhof-Parnas pathways. External enzyme activities showed that the 2,5-DKG pathway was very active. All enzyme activities were equivalent for cells in log growth and stationary phases. The low activity of the internal glucose metabolism pathways, coupled with a poor growth rate on glucose, and high activity of the 2,5-DKG pathway, suggested that most of the glucose is channeled

through the extracellular pathway. However, the portion of glucose entering central metabolism in *P. citrea* is significant and cannot be ignored when modeling the conversion of glucose to 2,5-DKG.

Batch experiments were performed to show the effect of central metabolism on the production of 2,5-DKG. Experiments performed with whole cells showed that approximately 75% of the glucose was converted to 2,5-DKG in 10 hours. Approximately 25% of the glucose was diverted to the central metabolic pathways. Experiments performed with French-pressed cells showed a 71% conversion of glucose in 11 hours. Experiments performed with permeabilized cells showed a 92% conversion of glucose in 18 hours. Although higher conversion of glucose was attained in the permeabilized cell case (91%) , the time taken to reach final conversion was much longer (17 hr) than that in the whole cell case (7 hr). The effect of the hydrodynamic shear (in the case of French-pressed cells) or chemical (toluene treatment in the case of permeabilized cells) treatments on the enzymes in the 2,5-DKG pathway remains unclear.

A model based on Michaelis-Menten kinetics of the three enzymes involved in the 2,5-DKG pathway was developed in order to predict the batch experimental 2,5-DKG profiles. The model consisted of a set of 4 coupled, nonlinear ordinary differential equations, each one describing the concentration of a species involved in the 2,5-DKG pathway. The input parameters needed were the volumetric activities of each of the three enzymes, glucosé dehydrogenase (E1), gluconate dehydrogenase (E2), and 2-KDG dehydrogenase (E3), cell density (X), and a glucose uptake rate constant, U_T. Of these parameters, only the volumetric E3 activity and cell density were measurable. The other

three parameters were determined by fitting the experimental data for one case of batch experiments performed with whole cells. These fit parameters were volumetric E1 activity = volumetric E2 activity = volumetric E3 activity, and U_T = 0.08 mmol/g/min. This model, with the fit parameters, successfully predicted the 2,5-DKG profile from another experiment with whole cells at a higher cell concentration, and therefore volumetric E1, E2, and E3 activities.

A sensitivity analysis on the adjustable parameters, volumetric E1 and E2 activities, and UT, revealed that small perturbations (±20%) did not affect greatly either the conversion (79%) of glucose to 2,5-DKG or the time required to reach that conversion. The overall conversion was most sensitive to perturbations in the volumetric E1 activity and U_T, and the time required to achieve the nominal conversion was most sensitive to the perturbations in the volumetric E2 activity.

Bibliography

Ameyama, M., K. Tayama, E. Shinagawa, K. Matsushita, and O. Adachi. *Agricultural Biological Chemistry*, 1981 45(4): 851-861

Ameyama, M., K. Tayama, E. Shinagawa, K. Matsushita, and O. Adachi. *Agricultural Biological Chemistry,* 1978, 42(12), 2347-2354.

Boston, M. Personal Correspondence, 1999.

Boudrant, J. *Enzyme Microb. Technol.*, 1990, 12, 322-329.

Chemical Profile. "Ascorbic Acid" http://www.chemexpo.com/news/profile981012.cfm 1999.

Chou, C., Bennett, G., and San, K. *Biotechnology and Bioengineering*, 1994, 44, 952-960.

Crawford, T. and Crawford, S. *Advances in Carbohydrate Chemistry and Biochemistry*, 1980, 37, 79-155.

Crawford, T.C. American Chemical Society, 1982. 1-36

Dalton, M. Personal Correspondence, 1999.

Gerhardt, P, Murray, R., Wood, W., Krieg, N. *Methods for General and Molecular Bacteriology*. ASM, Washington D.C., 1994.

Gottschalk, Gerhard. *Bacterial Metabolism. 2nd Ed.* Springer-Verlag, New York, 1986.

Kemerer, V.F., Griffin, C.C., and Brand, L. *Methods of Enzymology*, 1975, 42, 91-98.

Kulhanek, M. *Advances in Applied Microbiology*, 197012:11-33.

Lazarus, R.A., J. L. Seymour, R.K. Stafford, C.B. Marks, and S. Anderson. *Vitamin C: Bioconversion via a recombinant DNA approach. Genetics and Molecular Biology of Industrial Microoganisms*. Ed C.L. Hershberger, S.W. Queener, and G. Hegeman, 1989.

Lazarus, R.A., R.K. Stafford, J.L. Seeymour, M.S. Dennis, M.G. Lazarus, E.J.L. Hughes, H.I. Miller, C.B. Marks, and S. Anderson. *Metabolic and genetic aspects of a recombinant bioconversion leading to ascorbic acid. In Proceedings of the 6th International Symposium on Genetics of Industrial Microorganisms*. Edited by Heslot, H., J. Davies, J. Florent, L Bobichon, C. Durand and L. Penasse. 1073-1082. 1990

Lehninger, A. *Principles of Biochemistry*, Worth Publishing, New York, 1982.

Lessie, T., and Neidhardt, F.C. *Journal of Bacteriology,* 1967, 93: 1337-1345.

Matsushita, K., Ohno, Y, Shinagawa, E., Adachi, O, and Ameyama, M. Agricultural Biological Chemistry, 1980, 44(7), 1505-1512.

Mitamura, T., Urabe, I., and Okada, H. European Journal of Biochemistry, 1989, 186, 389-393.

Rippa, M., and Signorini, M.. *Methods of Enzymology*, 1975, 41, 237-240.

Shinagawa, E., Matsushita, K, Adachi, O, and Ameyama, M. Agricultural Biological Chemistry, 1981, 45(5), 1079-1085.

Sonoyama, T. and K. Kobayashi. *Journal of Fermentation Technolology* 1987, 65(3), 311-317.

Sonoyama, T., H. Tani, K. Matsuda, B. Kageyama, M. Tanimoto, K. K. Ashi, S. Yagi, H. Kyotani, K. Mitsushima. Applied and Environmental Microbiology, 1982, 43(5), 1064-1069.

Stryer, L. *Biochemistry*. 4th Ed. W.H. Freeman & Co., New York 1995.

White, David. *The Physiology and Biochemistry of Prokaryotes*. Oxford University Press, New York, 1995.

Wood, W.A., Fetting, R.A., and Hertlein, B.C. *Methods of Enzymology*, 1962, 5, 287-291.

VITA

Ziran Sun was born on July 9th, 1974 in Shanghai, People's Republic of China. He came to the United States of America on April 5th, 1985. He was enrolled into the 6th grade at East Rock Community School (New Haven, CT) where he received public secondary education. He graduated from Hopkins school (New Haven, CT) in June, 1992 where he received private high school education. He attended Cornell University (Ithaca, NY) and received a Bachelor of Science from the Department of Chemical Engineering in May, 1996. He then worked for Innovation Packaging Corporation (Rochester, NY) in July, 1996 as a statistical process engineer. He entered graduate school in August, 1997 at the University of Tennessee, Knoxville. In August, 1999, he will receive a Master of Science from the Department of Chemical Engineering. He will work for BASF Corp. as a Professional Development Program Engineer starting July, 1999.